REPORT DOCUMENTATION PAGE

Form Approved OMB No. 0704-0188

1. REPORT DATE *(DD-MM-YYYY)*	2. REPORT TYPE	3. DATES COVERED *(From – To)*
19-11-2001	Final Report	22 November 2000 - 04-Apr-02

4. TITLE AND SUBTITLE

Carrier dynamical approaches to SiGe Quantum Well devices

5a. CONTRACT NUMBER
F61775-01-WE007

5b. GRANT NUMBER

5c. PROGRAM ELEMENT NUMBER

6. AUTHOR(S)

Dr. Paul Harrison

5d. PROJECT NUMBER

5d. TASK NUMBER

5e. WORK UNIT NUMBER

7. PERFORMING ORGANIZATION NAME(S) AND ADDRESS(ES)

University of Leeds
School of Electronic and Electrical Engineers
Leeds LS2 9JT
United Kingdom

8. PERFORMING ORGANIZATION REPORT NUMBER

N/A

9. SPONSORING/MONITORING AGENCY NAME(S) AND ADDRESS(ES)

EOARD
PSC 802 BOX 14
FPO 09499-0014

10. SPONSOR/MONITOR'S ACRONYM(S)

11. SPONSOR/MONITOR'S REPORT NUMBER(S)
SPC 01-4007

12. DISTRIBUTION/AVAILABILITY STATEMENT

Approved for public release; distribution is unlimited.

13. SUPPLEMENTARY NOTES

14. ABSTRACT

This report results from a contract tasking University of Leeds as follows: The contractor will investigate methods of improving SiGe quantum well infrared photodetectors by applying carrier dynamics. The goal of the contractor's research will be to set the foundation for the development of Si-based focal plane arrays for active and passive imaging in the mid- and long-wave infrared.

15. SUBJECT TERMS
EOARD, Imaging, Photonics, terahertz technology, infrared technology, Quantum Well Devices

16. SECURITY CLASSIFICATION OF:			17. LIMITATION OF ABSTRACT	18, NUMBER OF PAGES	19a. NAME OF RESPONSIBLE PERSON
a. REPORT	b. ABSTRACT	c. THIS PAGE			David M. Burns, Lt Col, USAF
UNCLAS	UNCLAS	UNCLAS	UL	32	19b. TELEPHONE NUMBER *(Include area code)* +44 (0)20 7514 4955

Carrier dynamical approaches to SiGe quantum well infrared photodetectors: Final report

Contract: F61775-01-WE007

P. Harrison,
The Institute of Microwaves and Photonics,
The School of Electronic and Electrical Engineering,
University of Leeds, LS2 9JT, U.K.
e-mail: p.harrison@physics.org
http://www.ee.leeds.ac.uk/homes/ph/

November 6, 2001

Table of Contents

1 Introduction

In this special contract the carrier dynamical approaches to optoelectronic device design that were introduced and developed in the earlier contract (F61775-99-WE055) were to be applied to quantum well infrared photodetectors (QWIPs).

QWIPs are highly developed and very successful devices which operate across the wide range (4-14 μm) of the mid-infrared band [1–5]. The individual photodetectors themselves are relatively simple, often just consisting of a biased multiple quantum well stack [6–9]. Doping introduces carriers into the system, which gather in the quantum wells. Incident photons can ionize the carriers from the quantum wells and into the continuum levels, where they constitute a current which can be detected by an external circuit, see Fig. 1.

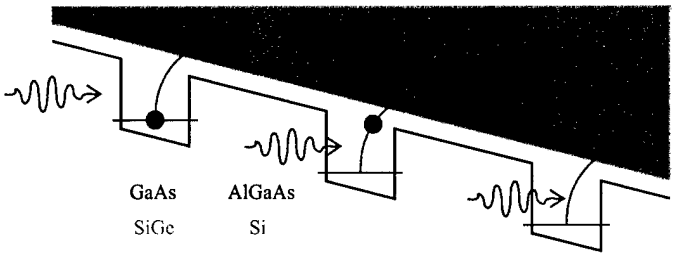

Figure 1: Schematic diagram showing the operation of a QWIP.

Arrays consisting of many thousands of individual photodetectors (pixels) have been demonstrated [10–14]. The latter has led to the development of full imaging systems, which although they require the focal-plane-array to be cooled to 77 K, which is achieved with a Stirling closed cycle cooler, have been minaturised to hand-held cameras weighing just a few kilograms [2, 4, 10, 14] and telescopes [3].

The motivation of this work was to explore the carrier dynamical issues for extending the detection wavelength to far-infrared ($> 20\ \mu$m) and even Terahertz ($> 30\ \mu$m) wavelengths.

References

[1] E. Dupont, H. C. Liu, M. Buchanan, Z. R. Wasilewski, D. St-Germaine, and P. Chevrette, 'Pixel-less infrared imaging based on the integration of an n-type quantum well infrared photodetector with a light-emitting diode', *Appl. Phys. Lett.*, **75**:563, 1999.

[2] S. D. Gunapala, S. V. Bandara, A. Singh, J. K. Liu, S. B. Rafol, E. M. Luong, J. M. Mumolo, N. Q. Tran, J. D. Vincent, C. A. Shott, J. Long, and P. D. LeVan, '8-9 and 14-15 μm two-color 640×486 GaAs/AlGaAs quantum well infrared photodetector (QWIP) focal plane array camera', in *Infrared Technology and Applications XXV*. SPIE Vol. 3698, 1999, p. 687.

[3] M.E. Ressler, J.J. Bock, S.V. Bandara, S.D. Gunapala, and M.W. Werner, 'Astronomical imaging with quantum well infrared photodetectors', *Infrared Phys. and Tech.*, **42**:377, 2001.

[4] M. Jhabvala, 'Applications of GaAs quantum well infrared photoconductors at the NASA/Goddard Space Flight Center', *Infrared Phys. and Tech.*, **42**:363, 2001.

[5] A. Zussman, B.F. Levine, J.M. Kuo, and J. de Jong, 'Extended long-wavelength λ=11–15μm GaAs/Al_xGa_{1-x}As quantum well infrared photodetectors', *J. Appl. Phys.*, **70**(9):5101, 1991.

[6] G. Sarusi, S.D. Gunapala, J.S. Park, and B.F. Levine, 'Design and performance of very long wavelength GaAs/Al_xGa_{1-x}As quantum well infrared photodetectors', *J. Appl. Phys.*, **76**(10):6001, 1994.

[7] S. Gunapala, G. Surasi, J. Park, T. Lin, and B. F. Levine, 'Infrared detectors reach new lengths', *Physics World*, **7**:35, 1994.

[8] Meimei Z. Tidrow, 'Device physics and state-of-the art quantum well infrared photodetectors and arrays', *Materials Sci. Eng. B*, **74**:45, 2000.

[9] B. F. Levine, 'Quantum well infrared photodetectors', *J. Appl. Phys.*, **74**:R1, 1993.

[10] S.D. Gunapala, S.V. Bandara, J.K. Liu, W. Hong, E.M. Luong, J.M. Mumolo, MJ. McKelvey, D.K. Sengputa, A. Singh, C.A. Shott, R. Caralejo, P.D. Maker, J.J. Bock, M.E. Ressler, M.W. Werner, and T.N. Krabach, 'Quantum well infrared photodetector research and development at jet propulsion laboratory', *SPIE*, **3379**:382, 1998.

[11] S. D. Gunapala, J. K. Liu, J. S. Park, M. Sundaram, C. A. Shott, T. Hoelter, T.-L. Lin, S. T. Massie, P. D. Maker, R. E. Muller, and G. Sarusi, '9-μm cutoff 256×256 GaAs/Al_xGa_{1-x}As quantum well infrared photodetector hand-held camera', *IEEE Trans. Elec. Dev.*, **44**:51, 1997.

[12] M. Walther, F. Fuchs, H. Schneider, J. Fleiβner, C. Schönbein, W. Pletschen, K. Schwarz, R. Rehm, G. Bihlmann, J. Braunstein, P. Koidl, J. Zeigler, and G. Becker, 'Electrical and Optical properties of 8-12 μm GaAs/AlGaAs Quantum well Infrared Photodetectors in 256 × 256 Focal Plane Arrays', in *Intersubband Transitions in Quantum Well: Physics and Devices*, Sheng S.Li and Yan-Kuin Su, Eds., Boston, 1998, Kluwer Academic Publishers.

[13] S. Bandara, S. Gunapala, J. Liu, E. Luong, J. Mumolo, M. McKelvy, and W. Hong, 'Quantum well infrared photodetectors for long-wavelength infrared applications', *SPIE*, **3436**:280, 1998.

[14] S. D. Gunapala, J. S. Park, G. Sarusi, T.-L. Lin, J. K. Liu, P. D. Maker, R. E. Muller, C. A. Shott, and T. Hoelter, '15-μm 128×128 GaAs/Al_xGa_{1-x}As quantum well infrared photodetector focal plane array camera', *IEEE Transactions on Electron Devices*, **44**:45, 1997.

2 Scientific output

In order to avoid duplication the author has chosen to attach other documents produced as part of this project as appendices, rather than merely reproducing their discussions here. Six pieces of tangible output have been produced in the twelve months duration of the project:

Journal Papers

1. M. A. Gadir, P. Harrison and R. A. Soref, *'The advantages of p-type and design methodologies for $Si_{1-x}Ge_x$ far-infrared (Terahertz) quantum well infrared photodetectors (QWIPs)'*, accepted for publication in Physica E
2. M. A. Gadir, P. Harrison and R. A Soref, *'Arguments for p-type $Si_{1-x}Ge_x$/Si quantum well photodetectors for the far and very-far (Terahertz) infrared'*, accepted for publication in 'Superlattices and Microstructures'.
3. M. A. Gadir, P. Harrison and R. A. Soref, *'Responsivity of quantum well infrared photodetectors (QWIPs) at Terahertz detection wavelengths'*, submitted to J. Appl. Phys.

Conference Proceedings

4. P. Harrison, M. A. Gadir, N. E. I. Etteh and R. A. Soref, *'The physics of THz QWIPs'*, accepted for publication in the Proceedings of the Ninth International Conference on Terahertz Electronics

Conference Presentations

5. M. A. Gadir, P. Harrison and R. A. Soref, *'The advantages of p-type and design methodologies for $Si_{1-x}Ge_x$ far-infrared (Terahertz) quantum well infrared photodetectors (QWIPs)'*, poster presentation at the Tenth International Conference on Modulated Semiconductor Structures, Linz, Austria, July 2001
6. P. Harrison, M. A. Gadir, N. E. I. Etteh and R. A. Soref, *'The physics of THz QWIPs'*, oral presentation at the Ninth International Conference on Terahertz Electronics, Charlottesville, Virginia, October 2001

3 Summary of Scientific output

A model to estimate the strength of the thermionic emission of carriers from quantum wells, which is the primary contributor to the dark (noise) current in QWIPs, was applied to a range of device designs of different detection wavelengths and different material characteristics. It was shown that the thermionic emission increases with temperature, for a fixed wavelength, and increases with wavelength for a fixed temperature.

In particular, at low temperatures the thermionic emission was proportional to the fourth power of the wavelength, although this did reduce to the square of the wavelength at room temperature. This indicates that extending the wavelength of QWIPs from the mid-infrared 4–14 μm, say, where they are currently very successful, to the far-infrared, is going to lead to large increases in the thermionic emission and hence the dark (noise) current.

One idea to counter this was to look at what might happen if materials other than the usual GaAs/AlGaAs structures were employed. This was implemented theoretically by simply considering the effect an increase of the effective mass of the charge carriers would have. It was found that the strength of the thermionic emission was inversely proportional to the effective mass. Thus, if *p*-type material was employed, were the hole effective mass can be up to 0.6 electron rest masses (as in GaAs and SiGe for example), then the thermionic emission would be an order of magnitude less than in an *n*-type GaAs structure of the same detection wavelength. This is strong evidence suggesting that far-infrared (>20 μm) QWIPs realised in *p*-type materials with carriers of higher effective mass will have a much reduced noise current than in *n*-type materials.

The work moved on to consider design of actual QWIPs of different wavelengths made from strain-balanced $Si_{1-x}Ge_x$ quantum wells, surrounded by Si barriers. It was found that the two parameters of quantum well width and alloy concentration of Ge were sufficient to be able to cover detection wavelengths from the short-wave mid-infrared ($\sim$3 μm) to wavelengths deep into the far-infrared ($\sim$60 μm) or Terahertz (5 THz) regions of the spectrum.

In contrast to the considerations of controlling the noise source in long wavelength QWIPs, the project also investigated the effect of extending the detection wavelength on the (signal) photocurrent. The photocurrent response of a general QWIP were studied. In such a device, the photocurrent generated per unit of incident light power depends on quantities such as the photocurrent gain and the quantum efficiency. In turn, the latter depend more fundamentally upon the width of the quantum well constituting the QWIP. As the detection wavelength is also dependent on the width of the quantum wells, then it was possible to derive a relationship linking the detection wavelength to the photocurrent gain and the quantum efficiency, and hence, to the photocurrent.

This relationship demonstrated that the photocurrent signal per incident photon saturates at detection wavelengths of around 20 μm and is then constant at wavelengths deep into the far-infrared (up to 50 μm). The implications of this are that the signal from a QWIP, when expressed as a current per incident photon, will be no worse for a far-infrared QWIP than it is for a mid-infrared device.

Thus, the overall conclusion for the project is, that efforts should be focussed on controlling the *dark current* in order to realise a far-infrared QWIP with an acceptable signal-to-noise ratio.

4 Future work: Contract F61775-01-WE088

One of the aims for the new contract is to look at how subsystems could be developed which utilise the SiGe QWIP technology that has been studied in the current program. The motivation behind this aim is to pave the way to develop compact, lightweight, low power, cheap, mid- and far-infrared detectors for remote sensing applications. Such a device may consist of an array of detectors, each tuned to a slightly different wavelength, in order that spectroscopic information may be obtained. This would allow for the identification of chemical and biological species, in a package that is small enough to be dropped by parachute and to remain undetectable by radar (it could be as small as a book). The system could have local processing power which could feed back information to a base station via a wireless link. A theatre would be protected by dropping a 'fence' of these units around sensitive areas.

5 Attachments

1. M. A. Gadir, P. Harrison and R. A Soref, *'Arguments for p-type $Si_{1-x}Ge_x$/Si quantum well photodetectors for the far and very-far (Terahertz) infrared'*, accepted for publication in 'Superlattices and Microstructures'.
2. M. A. Gadir, P. Harrison and R. A. Soref, *'Responsivity of quantum well infrared photodetectors (QWIPs) at Terahertz detection wavelengths'*, submitted to J. Appl. Phys.
3. P. Harrison, M. A. Gadir, N. E. I. Etteh and R. A. Soref, *'The physics of THz QWIPs'*, accepted for publication in the Proceedings of the Ninth International Conference on Terahertz Electronics

Article Submitted to Superlattices and Microstructures

Arguments for p-type $Si_{1-x}Ge_x$/Si quantum well photodetectors for the far and very-far (Terahertz) infrared

M. A. GADIR[1], P. HARRISON[1] AND R. A. SOREF[2]

[1]*IMP, School of Electronic and Electrical Engineering, The University of Leeds, LS2 9JT, U.K.*

[2]*Sensors Directorate, AFRL/SNHC, Air Force Research Laboratory, Hanscom Air Force Base, MA 01731, U.S.A.*

Abstract

An analysis, by a carrier scattering approach, of the thermionic emission contribution to the dark current is carried out in conventional bound-to-continuum quantum-well infrared photodetectors (QWIPs). It is found that the thermionic emission increases with increasing temperature or when extending the detection wavelength from mid- to far-infrared. Considering p-type instead of n-type material, however the increased effective mass decreases the thermionic emission. Designs for mid- and far-infrared p-type QWIPs based on the $Si_{1-x}Ge_x$/Si system are discussed for both normal and non-normal incident geometries.

KEYWORDS: ***** Keywords not supplied *****

1. Introduction

Quantum well infrared photodetectors (QWIPs) are emerging as a new and important technology for the semiconductor industry as they seem to be attractive for thermal imaging and sensing applications. The best known and most widely discussed are the n-type devices based on GaAs/AlGaAs, due to their good uniformity when grown over large areas. However, they require special surface relief structures (i.e. a grating or other optical coupling structure) to change the direction of the light's propagation due to their inability to absorb normal incident light. Whereas, the quantum mechanical selection rules for p-type QWIPs allow absorption of light which is propagating parallel to the surface normal of the device. In addition to good uniformity, the epitaxial growth and processing of SiGe alloys is compatible with Si microelectronics technology including on-chip integration of SiGe focal-plane arrays with Si readout circuits. This makes QWIPs based on this material worth pursuing [1–6].

Improving the QWIPs' performance depends fundamentally on minimizing the leakage (dark) current which plagues all light detectors. Three major factors contribute to the existence of the dark current. The first is the quantum mechanical tunneling from quantum well to quantum well

through the barrier layer. This *sequential tunneling* (STDC) is fairly independent of temperature and is thought to dominate below 30K. Secondly, there is thermally assisted tunnelling or *field induced emission* (FIEDC), which involves thermal excitation within the well followed by tunneling into the continuum. The final contribution is called *thermionic emission* (TEDC) in which there is direct excitation into the continuum band [2].

This paper will discuss some of the positive aspects associated with p-type QWIPs, and devices based on SiGe/Si, in some detail.

2. Theoretical approach and methods

Two approaches are taken to derive the electronic structure of the QWIP. In the first discussions on general QWIP properties, a single band Schrödinger equation was employed:

$$-\frac{\hbar^2}{2}\left(\frac{\partial}{\partial z}\frac{1}{m^*}\frac{\partial}{\partial z}\right)\psi(z)+V(z)\psi(z)=E\psi(z)$$

where $V(z)$ is the one-dimensional potential describing the heterostructure under the effective mass and envelope-function approximations. The eigenvalues E and wavefunctions $\psi(z)$ were obtained by a numerical shooting technique and the Fermi-Dirac distribution functions deduced for given carrier densities, see Harrison [7] for full derivations and source codes.

The later discussions of p-type SiGe QWIPs require a more sophisticated multi-band approach, and for this a commercial 8-band **k.p** calculation was used.

3. Advantages of p-type QWIPs for dark current

3.1. Effect of increased effective mass on sequential tunnelling and field induced emission

The dark current is the sum of three different carrier scattering contributions as mentioned by Gunapala and Etteh *et al* [2, 8]. Sequential tunnelling of carriers is well understood and is reduced by increasing the thickness of the barriers between the quantum wells constituting the QWIP. However it should be noted that sequential tunnelling could also be reduced by increasing the effective mass of the charge carrier - an effect that would occur normally if QWIPs were made from p-type rather than n-type material. A reduced barrier thickness would allow for either thinner devices or more (absorbing) quantum wells.

It is also recognized that field induced emission tends to be more significant at field strengths higher than typically found in working devices, thus the contribution of thermionic emission to the dark current appears to be the area where increasing the effective mass could produce the greatest benefits and for this reason this is where attention will be focussed.

3.2. Model for calculating thermionic emission

In order to evaluate the strength of the thermionic emission as a function of some parameters such as detection wavelength, effective mass and temperature, a simple model was constructed as shown in figure 1. Following Etteh[8], the thermionic emission was taken as proportional to the density of electrons, as given by Fermi-Dirac distribution function at the top of the well. This

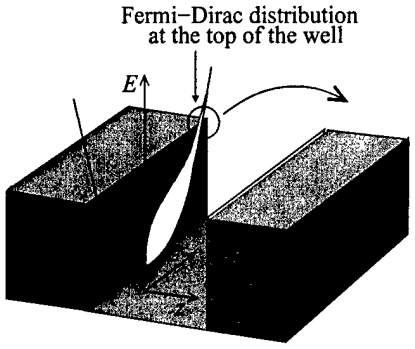

Figure 1: Thermionic emission mechanism in a quantum well

originates from the simple assumption that the more electrons near the top of the quantum well barrier, the more will be ionized and move into the continuum.

3.3. Effect of detection wavelength on thermionic emission:

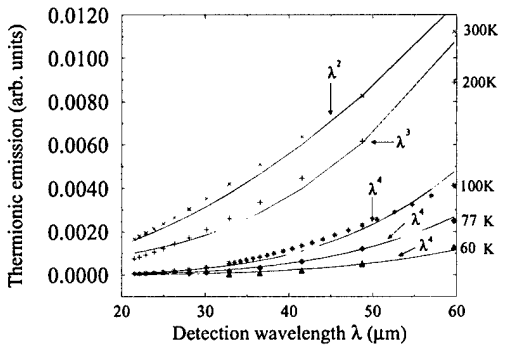

Figure 2: The relative strength of thermionic emission versus detection wavelength at $0.067m_o$ for different temperatures in a $GaAs/Ga_{0.9}Al_{0.1}As$ QWIP. Solid lines represent λ^2, λ^3 and λ^4 fits to the data

To illustrate the dark-current trends that are predicted using this model, we shall focus initially upon n-type GaAs/AlGaAs QWIPs. Then, in section 4, we shall extend our analysis to the p-type SiGe QWIP system. Using the figure 1 model, figure 2 shows that the thermionic emission dark current increases with increasing wavelength of the detected light (altered by changing the quantum well width, between 30 and 90Å at a fixed barrier width of 300Å) for temperatures of 60, 77, 100, 200 and 300K which results in the reduction of the photodetector's efficiency (signal to noise ratio). The behaviour of the thermionic emission when varying the detection wavelength at 100K could be fitted well with λ^4 curves (these are shown as solid lines in figure 2). It was verified that the dependency was quartic and not quadratic or cubic. Thus at 100K, the strength of thermionic emission is proportional to λ^4 (see figure 3 for different effective masses). This

dependency represents an obstacle that could obstruct the development of Terahertz (far-infrared) QWIPs. For example, doubling the detection wavelength of a QWIP from 20 μm to the edge of the THz band at 40 μm (15 to 7.5 THz), at common liquid nitrogen operating temperatures (77K), would drastically increase the strength of the thermionic emission by 16 fold.

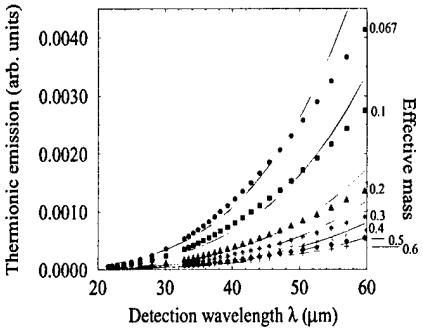

Figure 3: Relative strength of Thermionic emission versus Detection wavelength at 100K for different effective masses in a GaAs/$Ga_{0.9}Al_{0.1}$As QWIP. λ^4 is represented by the solid lines which are fitted to the data

The calculations were repeated at 200K and are plotted in figure 2. Again curve fitting was used to obtain:

$$\text{Thermionic emission} \propto \lambda^3$$

In figure 2, at 300K as the curves are (largely) parabolic, indicating a relationship of the form:

$$\text{Thermionic emission} \propto \lambda^2$$

3.4. Effect of effective mass on thermionic emission

In figures 2, after original calculations with the GaAs value of $0.067m_o$, the effective mass was increased and the effect on the Fermi-Dirac distribution function recalculated, see figure 3. It can be seen that for all detection wavelengths and all temperatures, increasing the effective mass of the carrier decreases the thermionic emission. Furthermore, the λ^4, λ^3 and λ^2 dependencies all hold.

Figure 4 inverts the earlier data and shows the relative strength of the thermionic emission versus the effective mass for several detection wavelengths. This demonstrates clearly that as the effective mass increases, the thermionic emission decreases. The solid lines show $1/m^*$ fits to the data, thus for any given wavelength:

$$\text{Thermionic emission} \propto \frac{1}{m^*}$$

3.5. Thermionic emission versus temperature

Expanding the investigation of thermionic emission strength as a function of temperature, figure 5 was produced. It could be seen that the relative strength of the thermionic emission for a fixed λ increases as T increases (linearly in approximation).

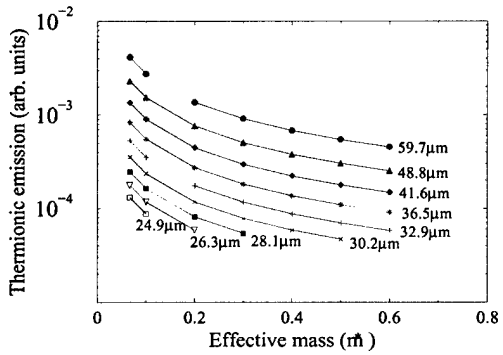

Figure 4: Thermionic emission versus effective mass at 100K for different detection wavelengths in a GaAs/$Ga_{0.9}Al_{0.1}$As QWIP. The solid lines represent $1/m^*$ fits the data

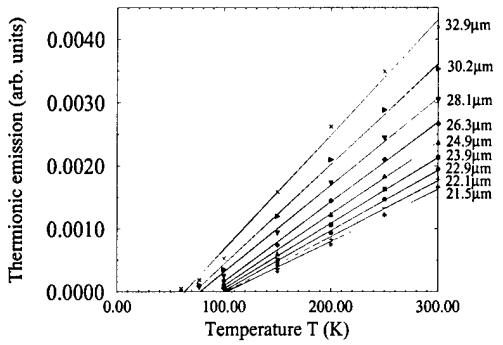

Figure 5: Thermionic emission versus temperature for different detection wavelengths at an effective mass of $0.067m_o$ for a GaAs/$Ga_{0.9}Al_{0.1}$As QWIP

3.6. Summary

The work in this section has shown that thermionic emission is going to be a problem when extending the wavelength of QWIPs from mid- to far-infrared. However, if the effective mass of the charge carrier, e.g. the electron, could be increased, by moving to p-type material where holes are the charge carriers, then much of this loss could be recouped. For example, in p-doped $Si_{0.8}Ge_{0.2}$ alloy quantum wells, the in-plane effective masses for light and heavy holes are greater than 0.462 m_o and 0.275 m_o respectively, at 77K. This is an alternative route to the non-uniform QWIP [9], and offers certain other advantages, see below.

4. Preliminary SiGe QWIP design

This section discusses a few of the design philosophies for p-type $Si_{1-x}Ge_x$/Si QWIPs, the energy levels of which were calculated using an 8-band **k.p** model (the finite-element software from Quantum Semiconductor Algorithms, Inc. of Northborough, MA). Starting with the heavy- to light-hole/split-off normal-incidence absorption without the need for a surface grating in

a bound-to-quasi-bound configuration, the work moves on to consider non-normal incidence heavy- to heavy-hole intra-band absorption.

4.1. Normal incidence, bound-to-quasi-bound

Various designs were examined for strain-balanced $Si_{1-x}Ge_x$/Si QWIPs grown upon a relaxed $Si_{1-y}Ge_y$ buffer-on-Si for several concentrations x of Ge. For a bound-to-quasi-bound configuration, it is essential to obtain one state in the p-doped well (as usual) and the other near the top of the well (i.e. quasi-bound taken to be within kT from the top of the well). In addition, normal incidence absorption requires a transition between two energy bands with different characters, for instance, heavy-hole to light-hole or split-off band. This is illustrated by dashed arrows in figures 6-9 which are the results of 8-band **k.p** calculations of the energy levels of $Si_{1-x}Ge_x$ quantum wells surrounded by Si barriers at 77K.

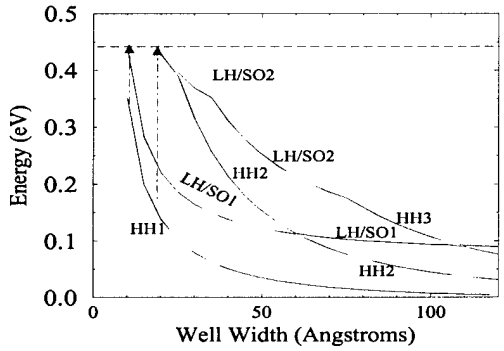

Figure 6: The 4 lowest Subband energies versus well width in a $Si_{0.4}Ge_{0.6}$/Si quantum well, the dashed vertical arrows show possible transitions for normal incidence absorption in the quantum well, and the horizontal dashed line shows the position of the HH bandedge in Si, the top of the quantum well

Figure 6 shows the 4 lowest energy levels for a $Si_{0.4}Ge_{0.6}$ quantum well as a function of well width at T=77K. For each choice of well width, the Si barrier width on each side of the well was chosen so that the average in-plane lattice constant of the SQW remained constant for each of the different Ge concentrations. This lattice constant is that of the $Si_{1-y}Ge_y$ buffer. The overall net in-plane strain of well-plus-barriers (compressive-plus-tensile) was zero in each case. Starting from a Si barrier of width 6.7Å for the 10.6 Å well width, the barrier width was increased to 80 Å as the well width increased to 120 Å . The character of each of the subbands is indicated in the figure. Note the change in character of the first excited state, from LH/SO for wells narrower than 60Å to HH for wells wider than 60Å . Similar changes are seen in figures 7-9. The possible bound-to-quasi-bound transitions for normal incidence absorption are pointed out using the dashed vertical arrows from the populated ground state (HH1) to the top of the well (LH/SO1 or LH/SO2). Clearly, it can be seen that there are two well widths that satisfy this criteria, that is, around 10.6 Å and 18.9 Å which correspond to detection wavelengths of 17.5 μm and 4.4 μm respectively. The former is an ultra-narrow well with a width of 10.6 Å which could

never be grown with any quality. On the other hand, the detection wavelength obtained for a 18.9 Å well offers great potential as a mid-infrared detector design.

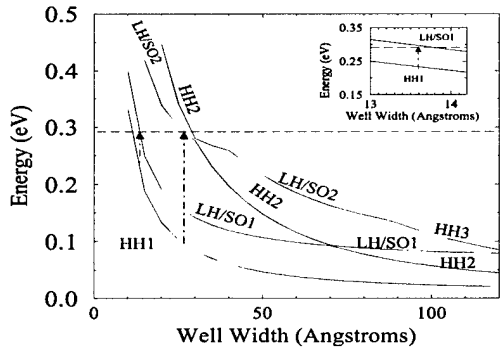

Figure 7: The 4 lowest Subband energies versus well width in a $Si_{0.6}Ge_{0.4}$/Si quantum well, the dashed vertical arrows show possible transitions for normal incidence absorption in the position of the HH bandedge in Si the top of the quantum well

Moreover, further calculations were performed for quantum wells with a 40% Ge concentration as shown in figure 7. Again arrows illustrate the procedure in which normal incidence could be obtained using a bound-to-quasi-bound transition. This again occurs approximately at a well width of 13.3 Å and also at 26.6 Å — the latter having a detection wavelength of 6.3 μm.

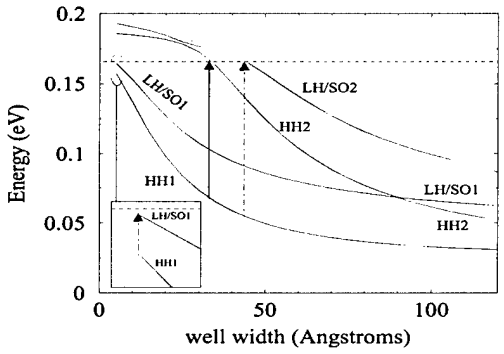

Figure 8: The 4 lowest Subband energies versus well width in a $Si_{0.8}Ge_{0.2}$/Si quantum well, the dashed vertical arrows show possible transitions for normal incidence absorption and a solid vertical arrow that illustrates a transition for non-normal incidence absorption in the position of the HH bandedge in Si the top of the quantum well

Moving to a lower concentration of germanium (i.e. $x = 0.2$), it can be seen in figure 8 that the potential depth is reduced compared to figure 7 and 6. Hence, the transition energies move to longer wavelengths, the bound-to-quasi-bound transitions take place in wells of width 5 Å and 43 Å . In the latter, HH1 to LH/SO2, the detection wavelength was evaluated to be 11.3 μm, illustrating this move to a longer wavelength with reduced Ge concentration.

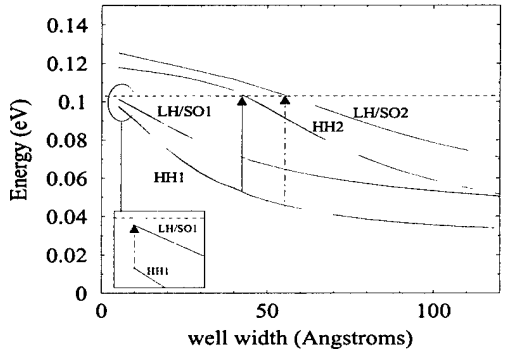

Figure 9: The 4 lowest Subband energies versus well width in a $Si_{0.9}Ge_{0.1}$/Si quantum well, the dashed vertical arrows show possible transitions for normal incidence absorption and a solid vertical arrow that illustrates a transition for non-normal incidence absorption in the position of the HH bandedge in Si the top of the quantum well

Finally, figure 9 was produced at 10% Ge concentration. The value of the well width, in which the bound-to-quasi-bound transition is indicated with a dashed arrow, has increased to around 55 Å with a corresponding detection wavelength of 21 μm which in commonly accepted terms is far-infrared.

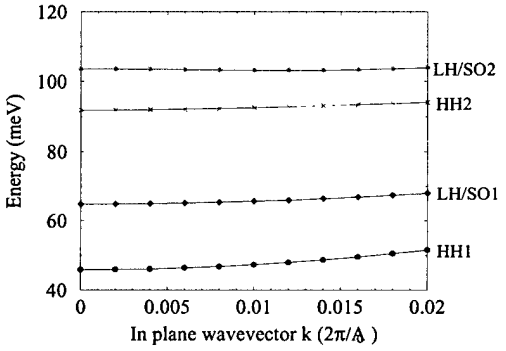

Figure 10: Energy versus in-plane momentum in a $Si_{0.9}Ge_{0.1}$/Si QWIP with a 55Å well width, at 77K

Figure 10 shows the subband dispersion for this 55 Å $Si_{0.9}Ge_{0.1}$/Si well, the non-parallel nature of the subbands involved in the bound-to-quasi-bound transition from HH1 to LH/SO2 is clear. Figure 11 shows this energy difference as a function of the in-plane wavevector k. This variation will lead to the photo-absorption peak becoming broader. For a hole density of $1 \times 10^{10}\text{cm}^{-2}$, calculations of the Fermi-Dirac distribution function suggests the photo-absorption peak might be broadened by 4 meV. This equates to 2 μm when centered around 21 μm. Interestingly, this design seems to be appropriate in terms of functionality and absorption, and suggests the exploration of low germanium concentrations which could be a most interesting area [10].

As a summary, decreasing the concentration x of germanium (as shown in the previous de-

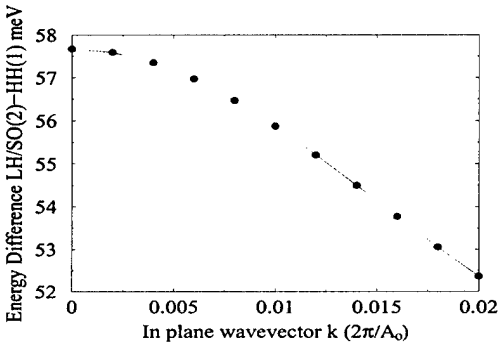

Figure 11: Energy difference between ground HH and the first excited LH/SO versus in-plane momentum in a $Si_{0.9}Ge_{0.1}$/Si QWIP with a 55Å well width, at 77K

signs) will increase the detection wavelength, therefore, enabling the construction of mid- and far-infrared $Si_{1-x}Ge_x$/Si QWIPs.

4.2. Non-normal incidence, bound-to-quasi-bound and bound-to-continuum

Non-normal incidence is also illustrated in figure 8 and 9 with the solid arrows representing the bound-to-quasi-bound transitions between two heavy-hole bands. The corresponding detection wavelength for a well of width 32 Å in figure 8 is 12.7 μm, again in the mid-infrared absorption region. At 42 Å in figure 9, a far-infrared detector could be designed with a 25 μm detection wavelength.

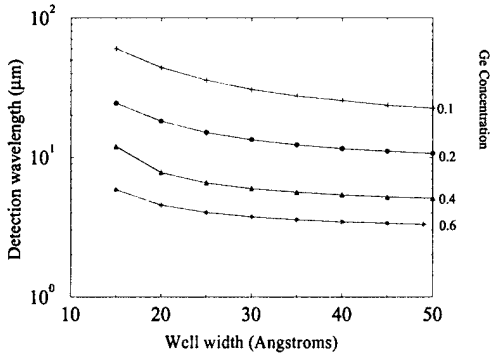

Figure 12: Detection wavelength versus well width for different Ge concentrations in the quantum well

In Figure 12, the curves illustrate the variation of the detection wavelength with the well width for different Ge concentrations at a temperature of 77K for straight forward bound-to-continuum absorption. It can be seen that the detection wavelength decreases (i.e. energy is increased) as the well width increases and as the Ge concentration increases, the data shows that bound-to-continuum non-normal incident QWIPs are possible with wavelengths from 3 μm in 50 Å $Si_{0.4}Ge_{0.6}$ quantum wells to 60 μm in 15 Å $Si_{0.9}Ge_{0.1}$ quantum wells.

5. Conclusion

The simple model which which has been used for estimating the strength of the thermionic emission dark current has shown that it increases with increasing detection wavelength and increasing temperature for bound-to-continuum QWIPs. In addition, thermionic emission could be reduced by increasing the effective mass of the charge carrier. This consideration suggests the importance of p-type QWIPs various designs of which were examined in the $Si_{1-x}Ge_x$/Si material system with an 8-band k.p model. It has shown that normal and non-normal incidence absorption detectors can be designed to operate in wavelengths spanning the mid and reaching into the far-infrared region in the spectrum.

Acknowledgments

The authors would like to thank the USAF European Office of Aerospace Research and Development(EOARD), grant reference F61775-01-WE007, for financial support.

References

[1] Burstein E. and Weisbuch C., editors. *Confined electrons and photons : new physics and applications*. New York London : Plenum Press, 1995.

[2] S. Gunapala, G. Sarusi, J. Park, T.L. Lin, and B. Levine. Infrared detectors reach new lengths. *Physics world*, 7(12):35–40, December 1994.

[3] S.D. Gunapala, S.V. Bandara, J.K. Liu, W. Hong, E.M. Luong, J.M Mumolo, M.J. McKelvey, D.K. Sengupta, A Singh, C.A. Shott, R. Carralejo, P.D. Maker, J.J. Bock, M.E. Ressler, M.W. Werner, and T.N. Krabach. Quantum well infrared photodetector research and development at jet propulsion laboratory. *SPIE Conference on Infrared Detectors and Focal Plane Arrays V*, 3379, April 1998.

[4] P. Kruck, A. Weichselbaum, M. Helm, T. Fromherz, and G. Bauer. Polarization-dependent intersubband absorption and normal-incidence infrared detection in p-type Si/SiGe quantum wells. *Superlattices and Microstructures*, 23(1), 1998.

[5] M.O. Manasreh, editor. *Semiconductor Quantum Wells and Superlattices for Long-Wavelength Infrared Detectors*. Artech House, INC., 1993.

[6] D.J. Robbins, M.B. Stanaway, W.Y. Leong, J.L. Glasper, and C. Pickering. $Si_{1-x}Ge_x$/Si quantum well infrared photodetectors. *Journal of materials science: Materials in Electronics*, 6:363–367, 1995.

[7] Paul Harrison. *Quantum Wells, Wires and Dots*. John Wiley & Sons, Chichester, 1999.

[8] N.E.I. Etteh and P. Harrison. Carrier scattering approach to the origins of the dark current in mid- and far-infrared (terahertz) quantum-well intersubband photodetectors (QWIPs). *IEEE Journal of Quantum Electronics*, 2001. To be published in May 2001.

[9] S.Y. Wang and C.P. Lee. Nonuniform quantum well infrared photodetectors. *Journal of Applied Physics*, 87(1):522–525, January 2000.

[10] R.A. Soref, L. Friedman, G. Sun, M.J. Noble, and L.R. Ram-Mohan. Quantum well Intersubband THz lasers and detectors. *SPIE Proceedings*, 3795(paper 80):1–12, July 1999.

The physics of THz QWIPs

P. Harrison, *Senior Member, IEEE*, M. A. Gadir, *Member, IEEE*, N. E. I. Etteh *Member, IEEE* and R. A. Soref, *Senior Member, IEEE*

Abstract— **In this work simple theoretical models are developed to explore the physics of quantum well infrared photodetectors (QWIPs) over a range of detection wavelengths spanning the mid- and far-infrared (Terahertz) regions of the spectrum. It has been shown that at low temperatures the dark current can vary as λ^4. However, a model of the wavelength dependence of the responsivity, which includes the effect of the quantum well width on the capture probability and quantum efficiency, suggests that the responsivity will be higher for the far-infrared wavelengths than it is for the mid-infrared.**

Keywords—**Terahertz, quantum well infrared photodetectors, qwip, far-infrared**

I. Introduction

QUANTUM Well Infrared Photodetectors (QWIPs) are highly developed and very successful devices which operate across the wide range (4-14 μm) of the mid-infrared band [1–5]. The individual photodetectors themselves are relatively simple, often just consisting of a biased multiple quantum well stack [6–9]. Doping introduces carriers into the system, which gather in the quantum wells. Incident photons can ionize the carriers from the quantum wells and into the continuum levels, where they constitute a current which can be detected by an external circuit, see Fig. 1.

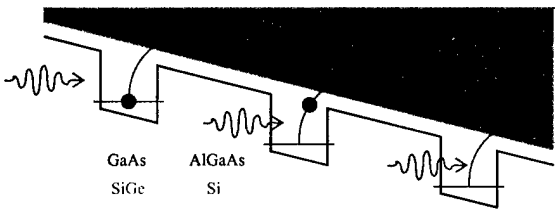

Fig. 1. Schematic diagram showing the operation of a QWIP.

Arrays consisting of many thousands of individual photodetectors (pixels) have been demonstrated [10–14]. The latter has led to the development of full imaging systems, which although they require the focal-plane-array to be cooled to 77 K, which is achieved with a Stirling closed cycle cooler, have been minaturised to hand-held cameras weighing just a few kilograms [2, 4, 10, 14] and telescopes [3].

The motivation of this work is to explore the possibility of extending the detection wavelength to far-infrared (> 20 μm) and even Terahertz (> 30 μm) wavelengths.

II. The dark current

It is the 'dark current', the current that flows even without the presence of incident light, which is the source of noise, and the main factor limiting the performance of QWIPs. Fig. 2 shows the three physical mechanisms which contribute to the ionization of carriers from the quantum wells *without photons*. Process (a), ground state sequential tunnelling, is basically propagated by carriers scattering from one quantum well to the next, by the emission of phonons or by carrier–carrier scattering. This process can be effectively shutdown (in mid-infrared devices) by making the barriers between the quantum wells very thick (of the order of several hundred Å).

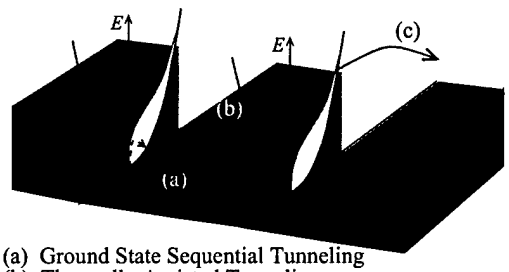

(a) Ground State Sequential Tunneling
(b) Thermally Assisted Tunneling
(c) Thermionic Emission

Fig. 2. The mechanisms contributing to the dark current.

The other two processes (b) thermally assisted tunnelling and (c) thermionic emission are basically manifestations of the same process. They effectively involve the ionization of carriers out of the quantum well by scattering with phonons and other carriers through the tip of the barrier or directly into the continuum, respectively.

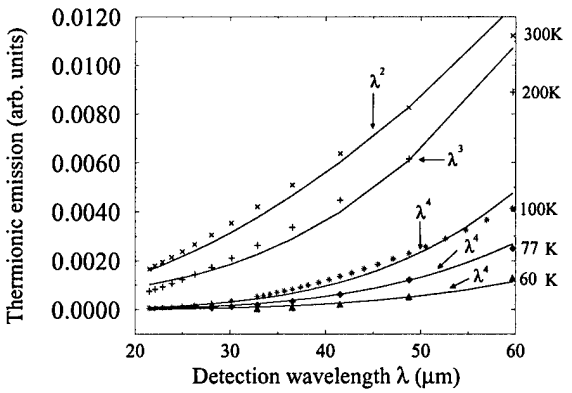

Fig. 3. Calculations of the thermionic emission as a function of the detection wavelength of a QWIP.

The detection wavelength of a QWIP is governed by the energy gap between the quantum well ground state and the top of the potential barrier. Hence, designing quantum wells for

Paul Harrison, Mazin Gadir and Nkaepe Etteh are at the Institute of Microwaves and Photonics, School of Electronic and Electrical Engineering, University of Leeds, LS2 9JT, U.K. E-mail: p.harrison@ee.leeds.ac.uk

Richard Soref is a member of the Sensors Directorate, AFRL/SNHC, Air Force Research Laboratory, Hanscom Air Force Base, MA 01731, U.S.A.

the detection of longer wavelengths implies narrowing the well (or making it shallower) such that this energy gap is reduced. Such a change, moves the carriers closer to the top of the well, where they become even more susceptible to phonon and carrier–carrier scattering and ionization from the well. Thus, it is easy to appreciate that increasing the detection wavelength of a QWIP leads to an increase in the dark (noise) current.

Simple calculations of the expected thermionic emission current from a QWIP as a function of the detection wavelength [15, 16] are shown in Fig. 3. It can be seen, in all cases, that as the detection wavelength λ increases the thermionic emission (i.e. the rate at which carriers leave the quantum wells) increases.

Curve fitting to the data shows that as the detection wavelength λ of a QWIP design is increased, the thermionic emission increases as λ^4 at low temperatures, λ^3 at mid-temperatures and λ^2 at room temperature. As the operating temperature of such devices is likely to be in the range of that of liquid nitrogen or below, it appears that the dark current could be the limiting factor in extending the detection wavelength from the mid- to the far-infrared.

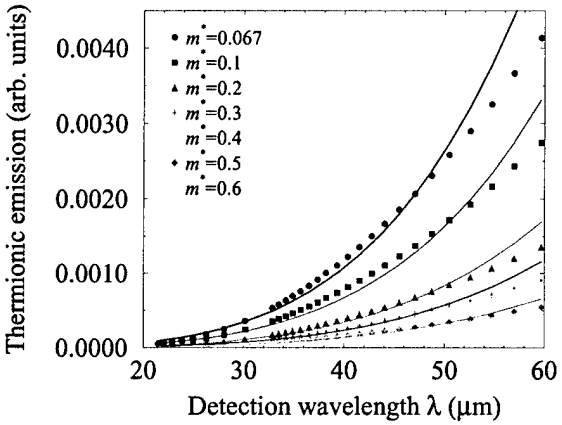

Fig. 4. Calculations of the thermionic emission as a function of the detection wavelength of a QWIP, for several different carrier effective masses m^*, at $T = 100$ K.

However, all is not lost. Fig. 4 shows the results of calculations of the thermionic emission strength at a temperature T of 100 K, for several different carrier effective masses. It can be seen that as the effective mass of the carrier (in this case the electrons) in the GaAs quantum wells is increased, the thermionic emission strength, and hence the dark current, decreases. This is because the increased density of states encourages the carriers to collect at the subband minimum and reduces the proportion of carriers which are in the thermal 'high-energy' tail of the Fermi-Dirac distribution. Hence, there are fewer carriers near the top of the well and the rate at which carriers are ionized from the well is reduced. This implies that the thermionic emission and resulting dark current may be reduced at any particular wavelength with the use of p-type (which generally has carriers with higher effective mass) rather than n-type material.

III. The Responsivity

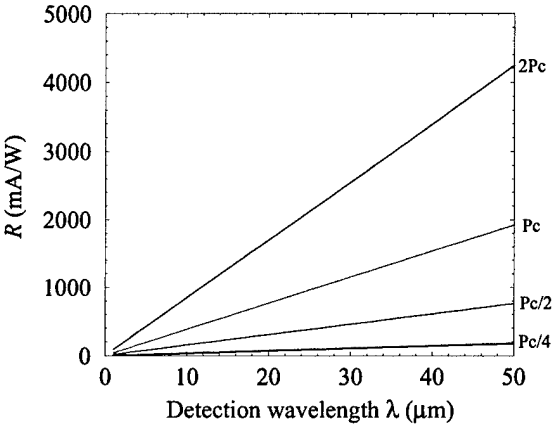

Fig. 5. The responsivity as a function of detection wavelength for a series of QWIP designs with the same number of periods and the same photoconductive gain.

The responsivity R is the photocurrent generated per unit of incident light power. It is defined as [17]:

$$R = \frac{e\eta}{hc}\lambda g \tag{1}$$

where the photoconductive gain g is defined as [9, 18]:

$$g = \frac{1 - P_c}{P_c}\frac{1}{N} \tag{2}$$

and η is the quantum efficiency [19], P_c is the capture probability and N is the number of quantum wells in the device.

It can be seen from equation 1 that for a fixed g, the responsivity R is proportional to the detection wavelength λ of a device. This is illustrated by the data plotted in Fig. 5, which is normalised to the responsivity of a $\lambda = 5\,\mu$m $Si_{0.64}Ge_{0.36}/Si$ $N = 10$ period QWIP [20], with $\eta = 0.1$ and the quoted value of P_c as 0.346.

This result may seem surprising, because it implies that the responsivity, i.e. the photocurrent signal, continues to increase as the detection wavelength of a QWIP is increased. This seems counter intuitive because it is normally expected that such a move to longer wavelengths will become more difficult and the devices will not perform to the same standard. However, it must be remembered that the responsivity is defined as the photocurrent (signal) per unit of incident light power, and as the wavelength λ increases, the energy of a single photon hc/λ decreases, i.e. there are more photons per unit of incident light power. More photons provides the opportunity for more carriers to be excited from the quantum well and hence, a larger photocurrent can be expected.

IV. The Capture Probability and Quantum Efficiency

Recent work [21] has shown that the detection wavelength λ is related to the quantum well width l_w by the relation:

$$\lambda = \frac{A}{l_w} \tag{3}$$

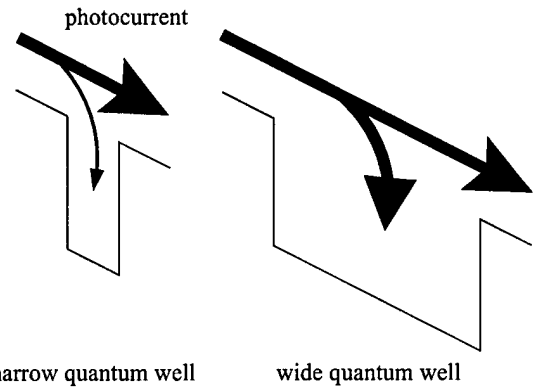

Fig. 6. Schematic diagram illustrating a possible effect of quantum well width on the capture probability.

The capture probability P_c is clearly a function of well width, and as suggested by Fig. 6, it would be expected that the wider the quantum well, the more likely a passing carrier would be recaptured. Gadir *et al.* [21] expressed this dependence as:

$$P_c = 1 - \exp\left(-\frac{l_w}{L_c}\right) \tag{4}$$

where L_c is some decay constant describing how quickly the capture probability changes as the well width increases. Given that the P_c is a function of quantum well width, and that the well width is a function of the detection wavelength then clearly the capture probability is not a constant and does indeed depend on λ.

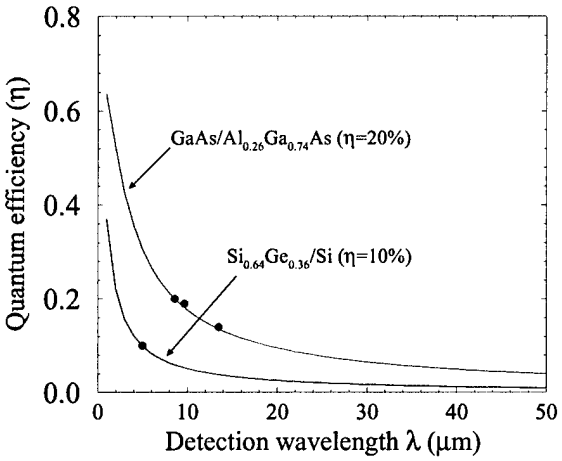

Fig. 7. The quantum efficiency η as a function of the detection wavelength λ, for an example GaAs/AlGaAs and a SiGe/Si QWIP. The solid points on the figure correspond to reported experimental data [20, 22].

Gadir *et al.* [21] also introduce a relationship for the well width dependence of the quantum efficiency:

$$\eta = \frac{2}{3}(1 - \exp(-\alpha N l_w)) \tag{5}$$

Given that λ has the functional dependence on the well width l_w in equation 3, then the quantum efficiency η can also be expressed in terms of λ. This functional dependency is shown in Fig. 7 for two example QWIP devices, one based in the GaAs/AlGaAs system [22](page 220 and 222) and one in the SiGe/Si system [20]. The GaAs/AlGaAs experimental data lies along the calculated line substantiating the theory. The value of the absorption coefficient α has been chosen such that the calculated curves pass through the reported values of η at the wavelengths of the real devices, i.e. $\eta = 0.2$ at $\lambda = 8.6\ \mu$m and $\eta = 0.1$ at $\lambda = 5\ \mu$m for the GaAs/AlGaAs and SiGe/Si devices respectively.

V. Responsivity at Far-Infrared Wavelengths

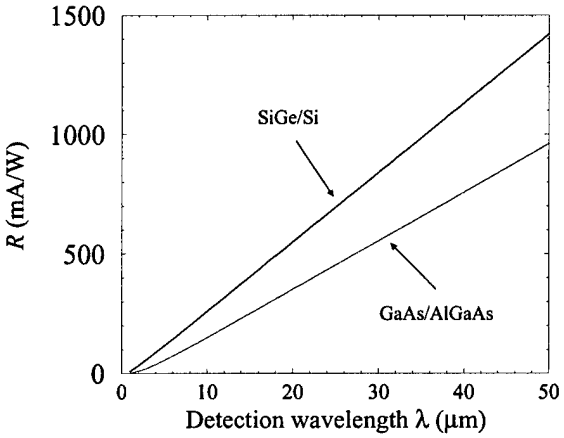

Fig. 8. The responsivity as a function of detection wavelength for a series of QWIP designs with the same number of periods, calculated including the well width dependencies of the capture probability and quantum efficiency summarised in equations 4 and 5.

Fig. 8 shows the effect on the responsivity, originally defined in equation 1, of including the wavelength dependencies of the capture probability and the quantum efficiency. It is interesting to note that these dependencies seem to almost cancel each other out and the functional form of the responsivity–wavelength data, in this more complete model, is identical to that of the earlier, simpler, calculations in Fig. 5. Although the proportionality is retained, the absolute values of the responsivity are reduced by around a factor of 2 (from the P_c case of Fig. 5). Note no significance should be attached to the fact that the *p*-type SiGe/Si device has a higher responsivity than the GaAs/AlGaAs device—these devices have different numbers of quantum wells, different doping densities and different biases.

As mentioned above, the true measure of the performance of a photodetector when considering devices designed for different detection wavelengths, may not be just in terms of the responsivity, but perhaps the photocurrent per *photon*. This is plotted, using the original data from Fig. 8, in terms of the number of photoelectrons, in Fig. 9. It can be seen that for both material systems the number of photoelectrons per photon reaches a plateau at detection wavelengths of around 10 μm and then remains constant as the wavelength is increased deep into the far-infrared and the Terahertz ($> 30\ \mu$m) regions of the spectrum.

This may seem a bizarre result—the standard responsivity and the photocurrent signal normalised to a single photon from a

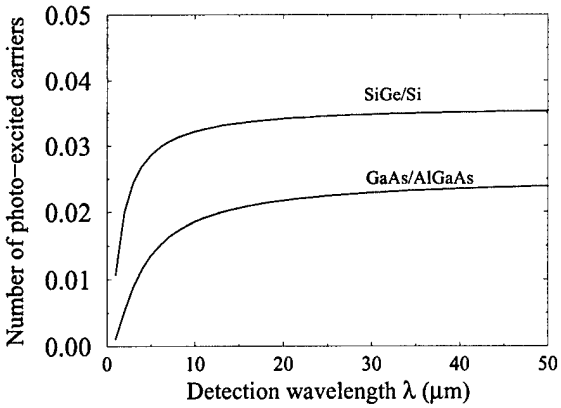

Fig. 9. The number of photoelectrons per incident photon as a function of the detection wavelength, for the example GaAs/AlGaAs and SiGe/Si devices.

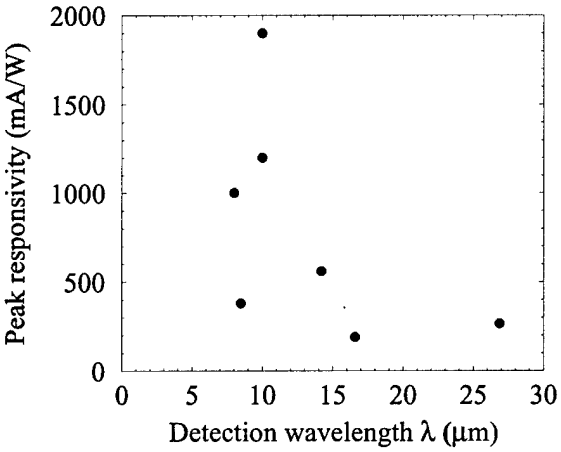

Fig. 10. The measured peak responsivity of a range of different GaAs/AlGaAs QWIPs [11, 14, 23–26].

QWIP is higher for far-infrared or Terahertz wavelengths than it is for the higher energy photons of the mid-infrared. However, this result is not disproved by currently available experimental data. Fig. 10 plots the peak responsivity from a range of reported devices. It can be seen there is no correlation at all between the responsivity and the wavelength. This probably relates to the different design configurations employed (different numbers of wells, different doping densities, differences in effectiveness of surface gratings etc.). To prove or disprove the conclusions found in this work, a consistent study is required, with a wide range of devices designed, grown and fabricated in succession using the same equipment and the same procedures.

VI. Summary

It has been shown that the responsivity (signal) of QWIPs may not be as bad as might be expected when the detection wavelength is increased. Indeed the work in this paper shows that the responsivity will increase as QWIPs are designed and fabricated to detect longer wavelengths—though it is acknowledged that overall device performance will decrease because of the increasing dark (noise) current. This suggests that the realisation of very long wavelength QWIPs might be more dependent upon controlling the dark current rather than the light current.

Acknowledgements

The authors would like to acknowledge financial support from the School of Electronic and Electrical Engineering, The University of Leeds and European Office of Aerospace Research and Development.

References

[1] E. Dupont, H. C. Liu, M. Buchanan, Z. R. Wasilewski, D. St-Germaine, and P. Chevrette, "Pixel-less infrared imaging based on the integration of an *n*-type quantum well infrared photodetector with a light-emitting diode," *Appl. Phys. Lett.*, vol. 75, pp. 563, 1999.

[2] S. D. Gunapala, S. V. Bandara, A. Singh, J. K. Liu, S. B. Rafol, E. M. Luong, J. M. Mumolo, N. Q. Tran, J. D. Vincent, C. A. Shott, J. Long, and P. D. LeVan, "8-9 and 14-15 μm two-color 640×486 gaas/algaas quantum well infrared photodetector (qwip) focal plane array camera," in *Infrared Technology and Applications XXV*. SPIE Vol. 3698, 1999, p. 687.

[3] M.E. Ressler, J.J. Bock, S.V. Bandara, S.D. Gunapala, and M.W. Werner, "Astronomical imaging with quantum well infrared photodetectors," *Infrared Phys. and Tech.*, vol. 42, pp. 377, 2001.

[4] M. Jhabvala, "Applications of gaas quantum well infrared photoconductors at the nasa/goddard space flight center," *Infrared Phys. and Tech.*, vol. 42, pp. 363, 2001.

[5] A. Zussman, B.F. Levine, J.M. Kuo, and J. de Jong, "Extended long-wavelength λ=11–15μm gaas/$al_xga_{1-x}as$ quantum well infrared photodetectors," *J. Appl. Phys.*, vol. 70, no. 9, pp. 5101, 1991.

[6] G. Sarusi, S.D. Gunapala, J.S. Park, and B.F. Levine, "Design and performance of very long wavelength gaas/$al_xga_{1-x}as$ quantum well infrared photodetectors," *J. Appl. Phys.*, vol. 76, no. 10, pp. 6001, 1994.

[7] S. Gunapala, G. Surasi, J. Park, T. Lin, and B. F. Levine, "Infrared detectors reach new lengths," *Physics World*, vol. 7, pp. 35, 1994.

[8] Mcimei Z. Tidrow, "Device physics and state-of-the art quantum well infrared photodetectors and arrays," *Materials Sci. Eng. B*, vol. 74, pp. 45, 2000.

[9] B. F. Levine, "Quantum well infrared photodetectors," *J. Appl. Phys.*, vol. 74, pp. R1, 1993.

[10] S.D. Gunapala, S.V. Bandara, J.K. Liu, W. Hong, E.M. Luong, J.M. Mumolo, MJ. McKelvey, D.K. Sengputa, A. Singh, C.A. Shott, R. Caralejo, P.D. Maker, J.J. Bock, M.E. Ressler, M.W. Werner, and T.N. Krabach, "Quantum well infrared photodetector research and development at jet propulsion laboratory," *SPIE*, vol. 3379, pp. 382, 1998.

[11] S. D. Gunapala, J. K. Liu, J. S. Park, M. Sundaram, C. A. Shott, T. Hoelter, T.-L. Lin, S. T. Massie, P. D. Maker, R. E. Muller, and G. Sarusi, "9-μm cutoff 256×256 gaas/$al_xga_{1-x}as$ quantum well infrared photodetector hand-held camera," *IEEE Trans. Elec. Dev.*, vol. 44, pp. 51, 1997.

[12] M. Walther, F. Fuchs, H. Schneider, J. Fleißner, C. Schönbein, W. Pletschen, K. Schwarz, R. Rehm, G. Bihlmann, J. Braunstein, P. Koidl, J. Zeigler, and G. Becker, "Electrical and optical properties of 8-12 μm gaas/algaas quantum well infrared photodetectors in 256 × 256 focal plane arrays," in *Intersubband Transitions in Quantum Well: Physics and Devices*, Sheng S.Li and Yan-Kuin Su, Eds., Boston, 1998, Kluwer Academic Publishers.

[13] S. Bandara, S. Gunapala, J. Liu, E. Luong, J. Mumolo, M. McKelvy, and W. Hong, "Quantum well infrared photodetectors for long-wavelength infrared applications," *SPIE*, vol. 3436, pp. 280, 1998.

[14] S. D. Gunapala, J. S. Park, G. Sarusi, T.-L. Lin, J. K. Liu, P. D. Maker, R. E. Muller, C. A. Shott, and T. Hoelter, "15-μm 128×128 gaas/$al_xga_{1-x}as$ quantum well infrared photodetector focal plane array camera," *IEEE Transactions on Electron Devices*, vol. 44, pp. 45, 1997.

[15] N. E. I. Ettch and P. Harrison, "Carrier scattering approach to the origins of dark current in mid- and far-infrared (terahertz) quantum-well intersubband photodetectors (qwips)," *IEEE J. Quan. Elec.*, vol. 37, pp. 672–675, 2001.

[16] M. A. Gadir, P. Harrison, and R. A. Soref, "Arguments for *p*-type sige/si quantum well photodetectors for the far and very-far (terahertz) infrared," *Superlatt. Microstruct.*, 2001, accepted.

[17] K.K. Choi, *The Physics of Quantum Well Infrared Photodetectors*, World Scientific Publishing Co. Pte. Ltd., 1997.

[18] B. F. Levine, A. Zussman, S. D. Gunapala, M. T. Asom, and J. M. Kuo ad W. S. Hobson, "Photoexcited escape probability, optical gain, and noise

in quantum well infrared photodetectors," *J. Appl. Phys.*, vol. 72, pp. 4429, 1992.

[19] H.S. Nalwa, Ed., *Handbook of Nanostructure Materials and Nanotechnology; Opyical Properties*, vol. 4, Academic Press, 2000, Interlibrary loan.

[20] P. Kruck, M. Helm, T. Fromherz, G. Bauer, J.F. Nutzel, and G. Abstreiter, "Medium-wavelenght, normal-incidence, *p*-type si/sige quantum well infrared photodetector with background limited performance up to 85 k," *Applied physics letters*, vol. 69, no. 22, pp. 3372–3374, November 1996.

[21] M. A. Gadir, P. Harrison, and R. A. Soref, "Responsivity of quantum well infrared photodetectors (qwips) at terahertz detection wavelengths," *J. Appl. Phys.*, 2001, submitted.

[22] H.C. Liu and F. Capasso, Eds., *Intersubband Transitions in Quantum Wells: Physics and Device Application 1; Semiconductors and semimetals*, vol. 62, Academic Press, 2000.

[23] K.-K. Choi, B.F. Levine, C.G. Bethea, J. Walker, and R.J. Malik, "Multiple quantum well 10μm gaas/al$_x$ga$_{1-x}$as infrared detector with improved responsivity," *Applied Physics Letters*, vol. 50, no. 25, pp. 1814–1816, June 1987.

[24] B.F. Levine, C.G. Bethea, G. Hasnain, V.O. Shen, E. Pelve, and R.R. Abbott, "High sensitivity low dark current 10μm gaas quantum well infrared photodetectors," *Applied Physics Letters*, vol. 56, no. 9, pp. 851–853, Feb. 1990.

[25] B.F. Levine, A. Zussman, J.M. Kuo, and J. de Jong, "19μm cutoff long-wavelength gaas/al$_x$ga$_{1-x}$as quantum-well infrared photodetectors," *Journal of Applied Physics*, vol. 71, no. 10, pp. 5130–5135, May 1992.

[26] A. G. U. Perera, W. Z. Shen, S. G. Matsik, H. C. Liu, M. Buchanan, and W. J. Schaff, "Gaas/algaas quantum well photodetectors with a cutoff wavelength at 28 μm," *Appl. Phys. Lett.*, vol. 72, pp. 1596, 1998.

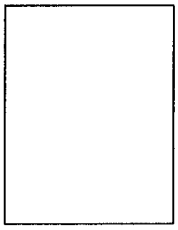

Paul Harrison graduated from the Universities of Hull and Newcastle upon Tyne with a BSc and PhD respectively in 1988 and 1991. From there he worked as a postdoctoral research assistant at the University of Hull until 1995 when he obtained a Fellowship at The University of Leeds. Since his attachment to the Institute of Microwaves and Photonics he has been working on ways to adapt his theoretical and computational experience in semiconductor heterostructures to Terahertz sources. Paul is now 'Reader in Quantum Electronics' and has authored two books, 'Quantum Wells, Wires and Dots' and 'Computational Methods in Physics, Chemistry and Biology'.

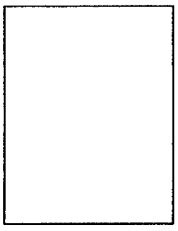

Nkaepe Etteh graduated from the University of Leeds in 1999 and is currently studying far-infrared (Terahertz) QWIPs as part of her PhD project.

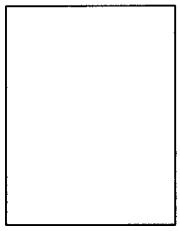

Mazin Gadir graduated from the University of Leeds in 2000 and is currently studying far-infrared (Terahertz) QWIPs, including SiGe implementations, as part of his PhD project.

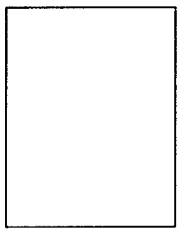

Richard A. Soref received the PhD degree in Electrical Engineering from Stanford University, Stanford, CA, in 1963.

He served as a Staff Member at MIT Lincoln Laboratory, Cambridge, MA, during 1963-1965, and was a Member of Technical Staff at Sperry Research Center, Sudbury, MA, from 1965 to 1983. In 1983 he joined the Air Force's Rome Air Development Center (now AFRL), Hanscom AFB, MA, where he is presently a Research Scientist in the Electromagnetics Technology Division of the Sensors Directorate. During these decades, he has contributed to electro-optical, guided-wave, and optical-microwave technology. Silicon-based optoelectronics, including quantum-well structures, has been his focus since 1986. He has authored or co-authored 180 journal articles and presentations, and has written six book chapters. Notable among his 24 invited talks are the 1998 lectures at the Fermi School in Varenna. He holds 46 U.S. patents.

Since 1983, Dr. Soref has managed AFRL research contracts, and is active in OSA, IEEE, and MRS conference organization, serving recently as Chairman of OSA's IPR-2000 Subcommittee on Dielectric Waveguides and as Co-Organizer of the Cross-connect Symposium. He was a Guest Editor of the IEEE Journal of Selected Topics in Quantum Electronics in 1998. He was awarded the U.S. Air Force Basic Research Award for pioneering work on semiconductor guided-wave optics in 1991, and is a Member of OSA, APS, MRS, SPIE, and a Fellow of AFRL.

Abstract category: D

The advantages of *p*-type and design methodologies for $Si_{1-x}Ge_x$ far-infrared (Terahertz) quantum well infrared photodetectors (QWIPs)

M. A. Gadir[1], P. Harrison[1] and R. A. Soref[2]

[1]*IMP, School of Electronic and Electrical Engineering, The University of Leeds, LS2 9JT, U.K.*
[2]*Sensors Directorate, AFRL/SNHC, Air Force Research Laboratory, Hanscom Air Force Base, MA 01731, U.S.A.*

This work is motivated by the desire to extend the operating wavelength of contemporary quantum well infrared photodetectors (QWIPs)[1] from the mid- ($< 14\mu$m) to the far-infrared ($> 20\mu$m) or Terahertz region of the electromagnetic spectrum without recourse to liquid helium temperatures[2]. This apparently simple objective hides many challenges which stem from the parasitic current that flows even in the absence of any illumination—the so-called *dark current*.

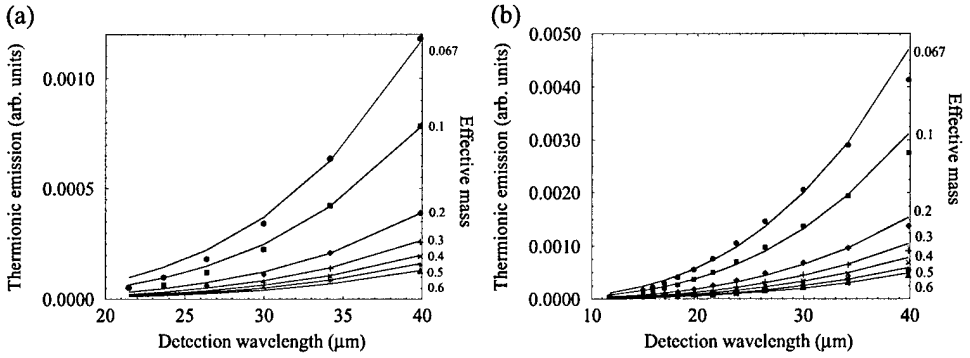

Figure 1: Calculations of the relative strength of the thermionic emission as a function of the detection wavelength (and for several different effective masses) for conventional bound-to-continuum $GaAs/Ga_{0.7}Al_{0.3}As$ QWIPs at (a) 100 K and (b) 300 K. The solid lines represent (a) λ^4 and (b) λ^2 fits to the data.

The dark current originates from three different carrier scattering processes[3]. Device designers have been able to effectively eliminate the contribution from sequential tunnelling of carriers from one quantum well into the next, and in addition, as field induced emission (ionisation) tends to be important only at fields higher than the typical operating conditions, then the major contributor to the dark current noise is from thermionic emission. The latter processes consists of thermal excitation of carriers out of the quantum well and increases with the temperature and as the bound state of the QWIP approaches the top of the barrier—as will need to occur if QWIPs are to work at longer wavelengths.

The calculated data in Fig 1 illustrates just how dramatic this increase in the thermionic emission is as a function of the detection wavelength λ of a device (varied by changing the quantum well width). In our model[3], the thermionic emission increases as λ^4 at 100 K, though interestingly this decreases to λ^2 at 300 K, see Figs. 1 (a) and (b) respectively. The λ^4 dependence at the common liquid nitrogen operating temperatures will be a major hindrance to the development of far-infrared (Terahertz) QWIPs.

One solution could be to increase the effective mass, m^*, of the charge carrier, which could mean considering *p*-type rather than the usual *n*-type material. The effect of increasing the effective mass, from the usual $0.067m_0$ for electrons in GaAs, is also shown in Fig. 1. This is summarised in Fig. 2(a)—for a fixed detection wavelength the thermionic emission contribution to the dark current varies as $1/m^*$.

Thus a move from n-type to p-type GaAs based devices could reduce the dark current by an order of magnitude—this would be one way to offset the increased noise as the detection wavelength of the devices is increased.

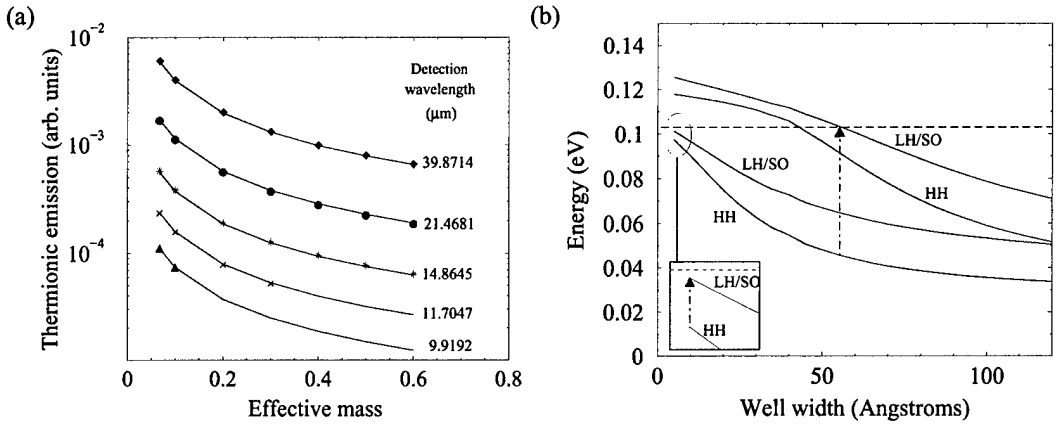

Figure 2: (a) Calculations of the relative strength of the thermionic emission as a function of the effective mass, for several different detection wavelengths, for GaAs/$Ga_{0.7}Al_{0.3}As$ quantum wells at 300 K. The solid lines are $1/m^*$ fits to the data and (b) 8-band **k.p** calculations of the subband structure of a strain-balanced $Si_{0.9}Ge_{0.1}$ quantum well surrounded by Si barriers, at 77 K. The letters (HH, LH and SO) indicate the character (heavy-hole, light-hole and split-off) of the subband at the zone centre.

A by-product of such a change in design philosophy would be the option of normal-incidence absorption, without the need for surface gratings, by employing a heavy- to light-hole interband absorption in a bound-to-quasibound configuration. Fig. 2(b) illustrates how this might be achieved in the $Si_{1-x}Ge_x$/Si material system. The figure shows example results of an 8-band **k.p** calculation of a strain-balanced multi-quantum-well (grown on a relaxed $Si_{1-y}Ge_y$ buffer) with a 10% Ge content surrounded by Si barriers. The arrows on the figure indicate that, for this Ge content, there are just two quantum well widths that produce light-hole subbands which are sufficiently close to the top of the well (as indicated by the dashed horizontal line) to be used in a bound-to-quasi-bound device. Inspection of the figure shows that these widths are at 5 and 55 Å which give detection wavelengths of 310 and 21 μm respectively.

Acknowledgements—The authors would like to thank the USAF European Office of Aerospace Research and Development (EOARD), grant reference F61775-01-WE007, for financial support.

References

[1] B. F. Levine, A. Zussman, S. D. Gunapala, M. T. Asom, and J. M. Kuo ad W. S. Hobson. Photoexcited escape probability, optical gain, and noise in quantum well infrared photodetectors. *J. Appl. Phys.*, 72:4429, 1992.

[2] A. G. U. Perera, W. Z. Shen, S. G. Matsik, H. C. Liu, M. Buchanan, and W. J. Schaff. GaAs/AlGaAs quantum well photodetectors with a cutoff wavelength at 28 μm. *Appl. Phys. Lett.*, 72:1596, 1998.

[3] N. E. I. Etteh and P. Harrison. Carrier scattering approach to the origins of dark current in mid- and far-infrared (terahertz) quantum-well intersubband photodetectors (QWIPs). *IEEE J. Quan. Elec.*, 2001. accepted.

Corresponding author: Mazin Gadir,
IMP, School of Electronic and Electrical Engineering,
The University of Leeds, LS2 9JT, U.K.
Tel: +44-113 233 2000 Fax: +44-113 244 9451
email: eenmag@leeds.ac.uk

Carrier dynamical approaches to SiGe quantum well infrared photodetectors: Mid-term report Contract: F61775-01-WE007

P. Harrison,
The Institute of Microwaves and Photonics,
The School of Electronic and Electrical Engineering,
University of Leeds, LS2 9JT

April 25, 2000

1 Introduction

In this special contract the carrier dynamical approaches to optoelectronic device design that were introduced and developed in the earlier contract (F61775-99-WE055) are to be applied to a type of photodetector based on semiconductor quantum wells. These detectors work on the principle of photons becoming absorbed and promoting carriers from localised states within quantum wells into the continuum where they can constitute a photocurrent, see Fig. 1. As the absorption transition is within a single band (and not a cross-bandgap absorption) these devices are sensitive to the lower energy photons of infrared light and are hence known as Quantum Well Infrared Photodetectors (QWIPs).

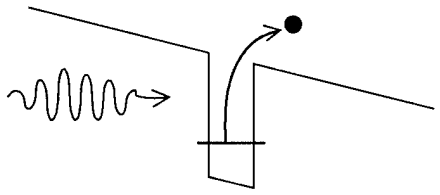

Figure 1: Operating principle behind a QWIP.

Arrays of QWIPs are being used as the active element in imaging systems, with applications in thermal imaging, night vision and astronomy. Traditionally the arrays are fabricated from *n*-type GaAs/AlGaAs heterostructures, however in this work *p*-type SiGe/Si layered structures are being considered. Although the material system is less mature, devices could offer beneficial properties

such as normal incidence absorption, reduced thermal noise, cheaper mass production and on-chip integration with standard Si electronics.

2 Summary of progress to date

- **Thermal noise:** QWIPs are very susceptible to thermal noise, which constitutes itself as an additional current which flows even in the absence of light. To combat this, traditional *n*-type devices are cooled, usually to around 70–80 K. A system made from such a device therefore suffers from increased weight, size and power consumption, all serious disadvantages if a portable imaging/scanning system is required.

  Moving to *p*-type material however, naturally increases the effective mass of the charge carriers which absorb the light, and the initial work in this project has shown that this will lead to a substantial decrease in the thermal noise.

- **Design configurations:** The use of *p*-type material also by-passes a quantum mechanical selection rule that *n*-type devices are constrained by, and allows for absorption of normal incidence light. Although solutions to deal with this issue are well known for *n*-type devices, removing this constraint allows for a simplification in the design. The latter half of the work completed so far has explored how the various energy transitions within $Si_{1-x}Ge_x$/Si heterostructures could be used to implement the traditional QWIP bound–to–quasi-bound and bound–to–continuum design configurations, see Fig. 2.

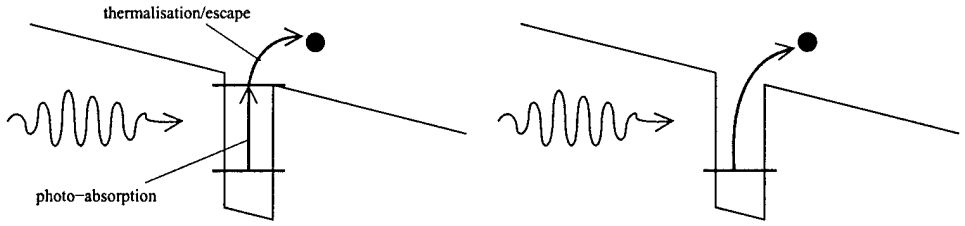

Figure 2: Bound–to–quasi-bound and bound–to–continuum approaches to engineering electron (or hole) transitions suitable for absorption of light and generation of a photocurrent.

3 Scientific output

In order to avoid duplication the author has chosen to attach other documents produced as part of this project as appendices, rather than merely reproducing their discussions here. Two pieces of tangible output have been produced in the six months that the project has been running:

1. M. A. Gadir, P. Harrison and R. A. Soref, *'The advantages of p-type and design methodologies for $Si_{1-x}Ge_x$ far-infrared (Terahertz) quantum well infrared photodetectors (QWIPs)'*, accepted for presentation at the 10th International Conference on Modulated Semiconductor Structures (MSS10), Linz, July 23-27 2001.

2. M. A. Gadir, P. Harrison and R. A Soref, *'Arguments for p-type $Si_{1-x}Ge_x$/Si quantum well photodetectors for the far and very-far (Terahertz) infrared'*, to be submitted to the international journal 'Superlattices and Microstructures'.

4 Future plans

- **Photocurrent calculation:** Calculation of the discrete energy levels of quantum wells allows designs for QWIPs to be forwarded, however the *performance* of these devices (sensitivity etc.) can only be deduced with more detailed consideration of the carrier dynamics, in particular an evaluation of the photo-response or the photo-current. Thus the major focus of attention for the latter half of this project will be the development of a model for the photo-current response of a $Si_{1-x}Ge_x$ QWIP. To achieve this a quantum mechanical scattering approach will be taken: Firstly to calculate the rate at which photo-carriers are generated—the carrier–photon scattering rate from the localised quantum well state summed over all continuum levels (similar to the process for calculating the thermionic emission contribution to the dark current as in a recent work [1]. Secondly, considering how this free carrier distribution reacts to the bias to form a current.

- **Carrier capture probability:** Many of the operating characteristics of real devices, such as photoconductive gain, responsivity and detectivity are dependent on a carrier dynamical property of the quantum well system known as the 'capture probability', see Fig. 3.

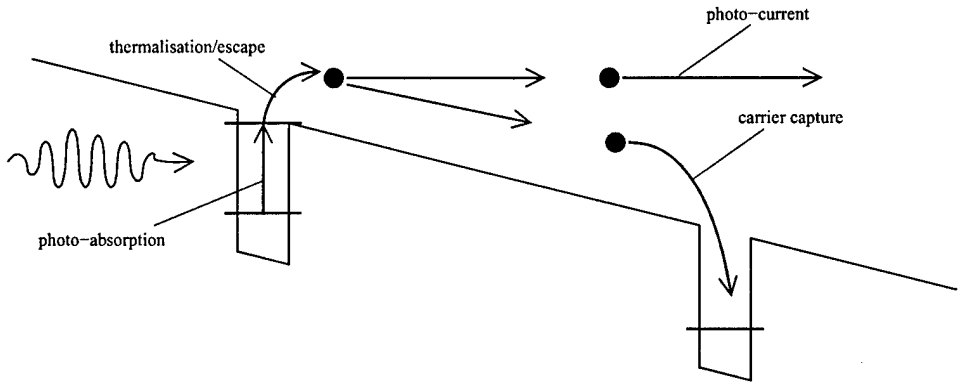

Figure 3: Typical photo-absorption processes in a QWIP, followed by the reduction in the photocurrent due to the recapture of a carrier by a neighbouring quantum well.

The second aim in the remainder of the project will be to investigate the effect the capture probability has on the characteristics of devices as their wavelength is extended from the mid- into the far-infrared, and to produce a roadmap for how this entity could be calculated—something which, to the author's knowledge, has never been achieved. Achieving this goal is likely to involve an extension or adaptation of the author's recent work on dark current calculations [1, 2].

With the work already done, completion of the above objectives should provide enough information to evaluate the potential of the $Si_{1-x}Ge_x/Si$ material system for long wavelength photodetectors. If these device designs look promising then this should provide leverage to persuade experimental partners to become involved in their development.

5 Project Timetable

Table 1: Work achieved so far in *italics*

Objective	Month											
	1	*2*	*3*	*4*	*5*	*6*	7	8	9	10	11	12
Literature review	*											
SiGe and QWIP familiarisation		*										
Simple model for thermionic emission			*									
Development of arguments for p-type				*								
Effect of increasing detection wavelength					*							
Initial SiGe device designs						*						
Interim report						*						
Calculations of photo-generated carrier distribution							*	*				
Response of carriers to electric field									*			
Design optimisation										*		
Investigations of effect of wavelength on capture probability											*	
Final report												*

References

[1] N. E. I. Etteh and P. Harrison, 'Full quantum mechanical scattering model of the dark current in quantum well intersubband photodetectors (QWIPs): The absence of sequential tunnelling and in-plane wave function decoherence', *IEEE J. Quan. Elec.*, 2001, to be submitted.

[2] N. E. I. Etteh and P. Harrison, 'Carrier scattering approach to the origins of dark current in mid- and far-infrared (Terahertz) quantum-well intersubband photodetectors (QWIPs)', *IEEE J. Quan. Elec.*, 2001, accepted.

Responsivity of quantum well infrared photodetectors (QWIPs) at terahertz detection wavelengths

October 11, 2001

M. A. Gadir and P. Harrison

IMP, School of Electronic and Electrical Engineering, The University of Leeds, LS2 9JT, U.K.

R. A. Soref

Sensors Directorate, AFRL/SNHC, Air Force Research Laboratory, Hanscom Air Force Base, MA 01731, U.S.A.

A first-principles model of the photocurrent in quantum well infrared photodetectors (QWIPs) is derived. The model examines the responsivity, carrier capture probability and quantum efficiency. It is found that the QWIP sensitivity reaches a plateau below the 10 μm detection wavelength and remains nearly constant from 10 to 50 μm.

Keywords: QWIP, photocurrent, capture probability, photoconductive gain, detection wavelength

1 Introduction:

QWIPs have attracted the attention of many researchers during the last decade [1–4], and the detailed physical understanding of QWIP operation has stimulated study of optimum QWIP design. This has resulted in the proposal of several theoretical models [5–8] to express primary QWIP characteristics such as responsivity, detectivity, photoconductive gain and photocurrent. However, the QWIP formulae derived from these different models vary due to the diversity in definitions and basic assumptions.

In this paper, a simplified unifying model is presented with the aid of some of the definitions and assumptions from the models mentioned above. It starts by defining the photocurrent in a simple detector and linking the physical characteristics of capture probability, gain and ultimately the responsivity, to the detection wavelength. The aim is to understand the consequences on the photocurrent of extending the detection wavelength of QWIPs to their far-infrared or terahertz limits.

2 Photocurrent and photoconductive gain:

Figure 1 shows a simple schematic diagram of a detector [9], where L is the thickness and A_d is the surface area of a slab of photoconductive material and Φ_s is the optical flux incident normally. The intensity of the flux is usually taken to decrease exponentially with the penetrating depth z [9], hence the intensity of flux at any depth z is:

$$\Phi(z) = \Phi_s(1-r)\exp(-\alpha z)$$

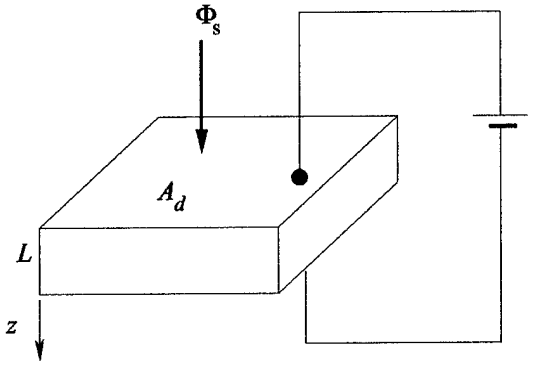

Figure 1: The geometry of a detector

where r is the reflection coefficient of the surface and α is the absorption coefficient of the material.

The photo-carrier generation rate per unit volume is given by [9]:

$$G(z) = -\frac{1}{A_d}\frac{\mathrm{d}\Phi(z)}{\mathrm{d}z}$$

$$\therefore G(z) = \frac{\alpha}{A_d}\Phi_s(1-r)\exp(-\alpha z)$$

At steady-state the photo-generated carrier density $P(z)$ is constant;

$$\text{i.e. } \frac{\partial P(z)}{\partial t} = 0$$

hence the generation rate must be equal to the recombination rate. Say the latter is described by a recombination lifetime τ, then

$$\frac{\partial P(z)}{\partial t} = G(z) - \frac{P(z)}{\tau} = 0$$

and hence:

$$P(z) = \tau G(z)$$

The average photo-electron density is therefore:

$$\bar{P} = \frac{1}{L}\int_0^L P(z)\,\mathrm{d}z = \frac{1}{L}\int_0^L G(z)\tau\,\mathrm{d}z = \frac{\Phi_s\tau}{\alpha L A_d}(1-r)\int_0^L \exp(-\alpha z)\,\mathrm{d}z$$

$$\therefore \bar{P} = \frac{\Phi_s\tau}{LA_d}(1-r)(1-\exp(-\alpha L)) = \eta\frac{\Phi_s\tau}{LA_d}$$

where η is known as the quantum efficiency and is defined here as the probability that a photon is absorbed in a quantum well to produce a photo-excited electron. This quantum well efficiency is shown below:

$$\eta = (1-r)(1-\exp(-\alpha l_w)) \tag{1}$$

where the absorbing length L is now taken as the width l_w of the quantum well [10]. Thus, αl_w. Recalling that a general current density is of the form 'nev', then the photocurrent

$$I_p = \bar{P}ev\ A_d \Longrightarrow I_p = (\eta\Phi_s)e\frac{\tau v}{L}$$

thus;

$$I_p = e\Phi_s\eta g \tag{2}$$

where g is known as the photocurrent gain and can be interpreted as the ratio of the electron mean free path τv to the sample thickness L and is interpreted as a measure of the photo-electron transport [9], [11]. The photoconductive gain is viewed in terms of a quantum well capture probability P_c and is derived from figure 2, see references [7], [10].

The total photocurrent consists of the remaining photocurrent (i.e. electrons not captured by the well) $(1-P_c)I_p$ and the emitted current from the well $(1-P_c)i_p$ [10], see figure 2. In order to maintain current continuity:

$$I_p = (1-P_c)I_p + (1-P_c)i_p$$

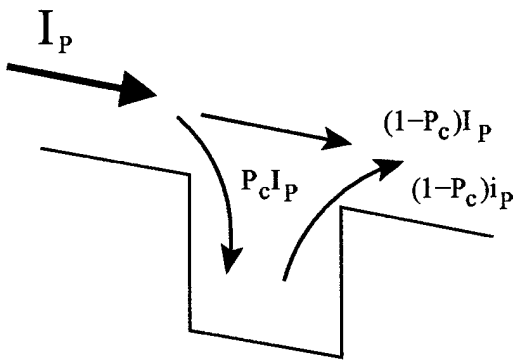

Figure 2: Schematic band diagram of a unit gain single well in a QWIP including the total net photocurrent I_p and the emitted photocurrent by a single well

$$\therefore I_p P_c = (1 - P_c) i_p$$

after using the definition in (2), I_p and i_p become [10]:

$$I_p = e\Phi_s \eta_n g \text{ and } i_p = e\Phi_s \eta$$

where η_n is the quantum efficiency of a number N of wells in a QWIP, and η is the quantum efficiency of a single well with unit gain. Now $P_c I_p = (1 - P_c) i_p$, therefore:

$$e\Phi_s \eta_n g P_c = (1 - P_c) e\Phi_s \eta$$

$$\therefore g = \frac{1 - P_c}{P_c} \frac{\eta}{\eta_n}$$

Recalling that $\eta_n = \eta N$, then:

$$g = \frac{1 - P_c}{P_c} \frac{1}{N} \tag{3}$$

as deduced by Levine *et al* [7], [10]

3 Responsivity:

The responsivity of a QWIP is a commonly used figure-of-merit for detector performance and is defined as the photocurrent per unit watt of incident light [9]; i.e.

$$R = \frac{e\eta g}{h\nu} \tag{4}$$

now,

$$\nu = \frac{c}{\lambda}$$

thus, in terms of wavelength λ,

$$R = \frac{e\eta g}{hc}\lambda \tag{5}$$

Taking the photoconductive gain g from equation (3), then:

$$R = \frac{e\eta}{hc}\lambda\frac{1-P_c}{P_c}\frac{1}{N} \tag{6}$$

Using this expression, figure 3 illustrates the responsivity R as a function of detection wavelength λ, for various, but fixed, capture probabilities P_c. It can be seen that there is a direct proportionality between R and λ. The standard capture probability P_c of 0.346 was taken from the 5 μm $Si_{0.64}Ge_{0.36}$/Si QWIP of reference [12], and the absolute values of the responsivity were calculated assuming a constant quantum efficiency η of 10% which is typical of many n- and p-type devices [7], [12], [13]. The number of wells in figure 3 was fixed at N=10.

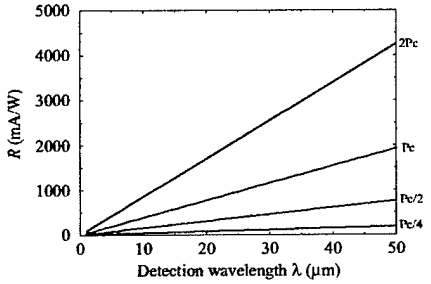

Figure 3: Responsivity versus detection wavelength for a range of capture probabilities P_c that are independent of λ. The reference value for P_c of 0.346 was taken from reference [12]

4 Capture Probability:

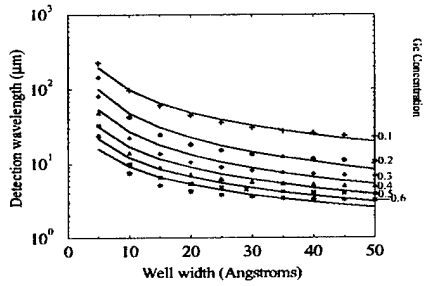

Figure 4: Detection wavelength λ versus well width l_w for different Ge concentration with fitted curves

Figure 4 shows the results of calculations [14] of the detection wavelength λ versus the quantum well width l_w for a series of $Si_{1-x}Ge_x$/Si quantum wells. The solid lines show curves fitted via A and B to the data of the form:

$$\lambda = \frac{A}{l_w^B} \tag{7}$$

It was found that the exponent B was always very close to 1, thus for the purpose of this work:

$$\lambda = \frac{A}{l_w} \tag{8}$$

with the parameter A (having the dimensions of cm^2) depending on the depth (in this case,

the Ge concentration x) of the well. The $Si_{0.64}Ge_{0.36}$/Si QWIP [12] mentioned earlier, is to be used as an example device configuration. For this material concentration, it was found that the constant A linking the wavelength λ and the quantum well width l_w (as in equation (8)) was $2.248 \times 10^{-10}cm^2$. The $GaAs/Ga_{0.74}Al_{0.26}As$ material system employed in the QWIPs of reference [15] will also be used. In this case A was found to be $4.83 \times 10^{-10}cm^2$.

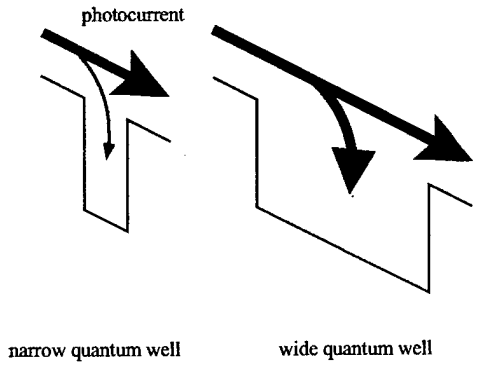

Figure 5: Schematic illustration of the proportion of the photocurrent which is captured by subsequent quantum wells

In the previous section the capture probability was assumed to have no dependence on λ, however it would be expected in practice that the capture probability increases with increasing well width, as illustrated with the aid of the arrow thickness in each well in figure 5. There are two important limits:

$$P_c \longrightarrow 0 \text{ as } l_w \longrightarrow 0$$

and

$$P_c \longrightarrow 1 \text{ as } l_w \longrightarrow \infty$$

Both of these limits could be fitted empirically by taking the capture probability as:

$$P_c = 1 - \exp\left(\frac{-l_w}{L_c}\right) \tag{9}$$

where L_c is a decay constant defining the rate of increase of the capture probability P_c with well width l_w. Using the expression for the wavelength dependence on the well width (equation (8)), then the capture probability can be expressed in terms of λ, i.e.

$$P_c = 1 - \exp\left(\frac{-A}{L_c\lambda}\right) \tag{10}$$

Now substituting equation (10) into (6) gives a relationship between the responsivity and the detection wavelength which includes this simple model for the capture probability. Thus the responsivity becomes:

$$R = \frac{e\eta}{hcN} \times \lambda \times \frac{\exp\left(\frac{-A}{L_c\lambda}\right)}{1 - \exp\left(\frac{-A}{L_c\lambda}\right)} \tag{11}$$

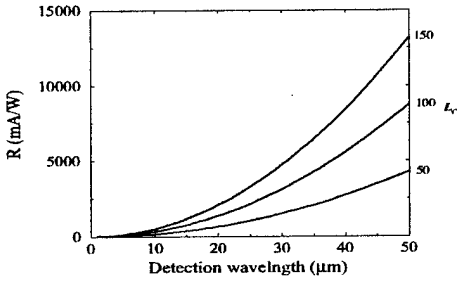

Figure 6: Responsivity as a function of detection wavelength for a varying capture probability ($L_c = 50, 100, 150$Å) as defined in equation (10). The other parameters are from reference [12], $N = 10$, and $A = 2.248 \times 10^{-10}$cm^2 for a Ge concentration of $x = 0.3$ with the quantum efficiency η kept constant at 0.10.

With the aid of equation (11), figure 6 re-plots the data of figure 3 (with the capture probability P_c scaled so that $P_c = 0.346$ when $\lambda = 5\mu$m) to display R as a function of λ for several

of the lengths L_c. It can be seen that the responsivity *increases* superlinearily with detection wavelength. This is because under this model the capture probability decreases with increasing wavelength, thus increasing the photoconductive gain g.

5 Quantum efficiency:

To improve the model still further, focus is now redirected towards the well quantum efficiency η which has been taken as constant. In reference [11], this quantum efficiency is defined as:

$$\eta = P(1-r)(1-\exp(-B\alpha l_w)) \tag{12}$$

where P is a polarization dependent constant ($P = 1$ for p-type QWIPs), α is the absorption coefficient and B is a constant depending on the number of paths the infrared radiation made through the QWIP active region. In the worst case of a semiconductor/air reflection coefficient $r = 1/3$ and $B = 1$, the quantum efficiency η would become:

$$\eta = \frac{2}{3}(1-\exp(-\alpha N l_w)) \tag{13}$$

where, in an N well device, Nl_w is the total width of absorbing material. Using the relationship between the well width and the detection wavelength given in equation (8), we get:

$$\eta = \frac{2}{3}(1-\exp\left[-\alpha N\frac{A}{\lambda}\right]) \tag{14}$$

The absorption coefficient α depends on the material system and the doping density. From reference [12], we obtain $\alpha = 36.15 \times 10^3 \text{cm}^{-1}$ for those particular 10 $Si_{0.64}Ge_{0.36}$/Si quantum wells which are homogeneously doped with boron giving a sheet concentration of $p_s =$

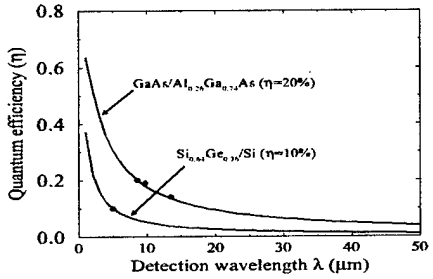

Figure 7: Quantum efficiency as a function of detection wavelength for the example material systems [12], [15]

$1.2 \times 10^{12}\text{cm}^{-2}$. Whereas, from [15] $\alpha = 25.4 \times 10^{3}\text{cm}^{-1}$ for the 25 period $\text{GaAs/Al}_{0.26}\text{Ga}_{0.74}\text{As}$ QWIP with a doping density $N_D = 1.4 \times 10^{18}\text{cm}^{-3}$ and surface grating to allow normal incidence. Then, substituting these values into equation (14), we obtain the η curves shown in figure 7. Then, returning to equation (11) we calculated the effect of the wavelength dependent quantum efficiency η summarised in equation (14) upon the responsivity-versus-wavelength relationship, but this time reverting back to the case of constant capture probability (see figure 8).

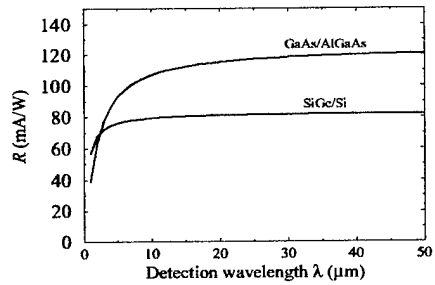

Figure 8: Responsivity as a function of detection wavelength for a constant capture probability and a variable quantum efficiency in SiGe/Si and GaAs/AlGaAs quantum wells. $L_c = 150\text{Å}$

6 Complete model:

Figure 9 shows the behaviour of the responsivity when both the capture probability and the quantum efficiency are allowed to be functions of the detection wavelength. We substituted equation (14) into equation (11) as shown in equation (15), thus completing the model.

$$R = \frac{e}{hcN} \times \lambda \times \frac{\exp\left(\frac{-A}{L_c\lambda}\right)}{1 - \exp\left(\frac{-A}{L_c\lambda}\right)} \times \frac{2}{3}\left(1 - \exp\left[-\alpha N \frac{A}{\lambda}\right]\right) \tag{15}$$

In figure 9 we took $A = 2.248 \times 10^{-10}\text{cm}^2$ and $N = 10$ as for the SiGe devices of reference [12] and $A = 4.83 \times 10^{-10}\text{cm}^2$ and $N = 25$ as for the GaAs/AlGaAs devices of reference [15]. It can be seen that there is almost a direct proportionality, mirroring the simple constants-based model at the beginning of this work. However the absolute magnitudes of the responsivity are now more justified. Further consideration needs to be given to this data because although the responsivity increases with detection wavelength, it does not tell the full story. The unit of the responsivity is milliAmps per watt with the latter representing the incident power. As the detection wavelength increases the photon energy decreases, hence there are more photons per watt, which may be expected to produce more photoelectrons and thus more photocurrent.

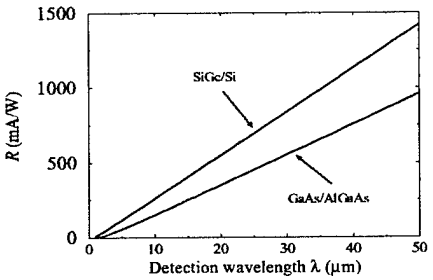

Figure 9: Responsivity as a function of detection wavelength for a variable capture probability and quantum efficiency (as a function of detection wavelength). L_c=150Å

In effect,

$$R = \frac{I_p}{P}$$

where I_p is defined in equation (2) and the incident power is:

$$P = N_p h\nu = N_p \frac{hc}{\lambda}$$

N_p is the number of photons per second. Hence, the complete photocurrent I_p equation becomes:

$$I_p = R \times P = N_p \frac{e}{N} \times \frac{\exp\left(\frac{-A}{L_c \lambda}\right)}{1 - \exp\left(\frac{-A}{L_c \lambda}\right)} \times \frac{2}{3}\left(1 - \exp\left[-\alpha N \frac{A}{\lambda}\right]\right) \tag{16}$$

Figure 10 shows the photocurrent per incident photon ($N_p = 1$) as expressed in equation (16).

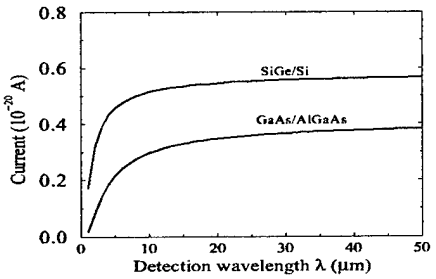

Figure 10: Photo-current as a function of detection wavelength when the power is 1 photon per second. $N_p = 1$

This is perhaps more vividly illustrated in figure 11 where the current is now given in terms of the number of photo-excited electrons per second:

$$\text{Number of photo-excited electrons} = \frac{I_p}{1.6 \times 10^{-19} C} \tag{17}$$

Both figures show that in these terms the sensitivity of the QWIPs reaches a plateau and for increasing wavelength a constant number of electrons can be expected to be photoexcited

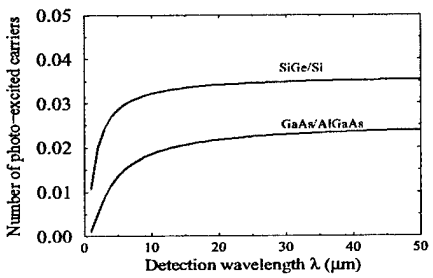

Figure 11: The number of photo-excited electrons as a function of detection wavelength when the power is 1 photon per second

per incident photon. (It maybe disconcerting to see SiGe QWIPs with 10% quantum efficiency having higher responsivity than 20% efficient GaAs/AlGaAs QWIPs. No significance should be attached to this, because the devices have different numbers of quantum wells and different doping densities, etc.)

7 Conclusion:

This paper has derived two essential relationships for the capture probability and the quantum efficiency, each one as a function of the detection wavelength. These dependencies have enabled the responsivity to be expressed in terms of the detection wavelength. Subsequently, a photocurrent model was established by focusing on the remaining factor: the incident power (i.e. $P = \frac{I_p}{R}$). As the latter was restricted to the power of a single photon, then the number of photo-excited electrons (to produce the photocurrent) was determined. It was found that the number of photoelectrons per incident photon is likely to tend towards a constant as the wavelength of the incident light is increased beyond 10μm and into the Terahertz region of the spectrum. This is an encouraging result and suggests that far-infrared QWIPs may have a sensitivity no less than

those in the mid-infrared region. The realisation of such devices will therefore be dependent upon control of the dark current in order to obtain a viable signal-to-noise ratio [14], [16–19].

References

[1] S.D. Gunapala, S.V. Bandara, J.K. Liu, W. Hong, E.M. Luong, J.M Mumolo, M.J. McKelvey, D.K. Sengupta, A Singh, C.A. Shott, R. Carralejo, P.D. Maker, J.J. Bock, M.E. Ressler, M.W. Werner, and T.N. Krabach. Quantum well infrared photodetector research and development at jet propulsion laboratory. *SPIE Conference on Infrared Detectors and Focal Plane Arrays V*, 3379, April 1998.

[2] S. Gunapala, G. Sarusi, J. Park, T.L. Lin, and B. Levine. Infrared detectors reach new lengths. *Physics world*, 7(12):35–40, December 1994.

[3] P. Kruck, A. Weichselbaum, M. Helm, T. Fromherz, and G. Bauer. Polarization-dependent intersubband absorption and normal-incidence infrared detection in p-type Si/SiGe quantum wells. *Superlattices and Microstructures*, 23(1), 1998.

[4] D.J. Robbins, M.B. Stanaway, W.Y. Leong, J.L. Glasper, and C. Pickering. $Si_{1-x}Ge_x$/Si quantum well infrared photodetectors. *Journal of materials science: Materials in Electronics*, 6:363–367, 1995.

[5] B.F. Levine. Device physics of quantum well infrared photodetectors. *Semiconductor science and technology*, 8:S400–S405, 1993. Invited paper.

[6] C. H. Liu. Photoconductive gain mechanism of quantum-well intersubband infrared detectors. *Applied Physics Letters*, 60(12):1507–1509, March 1992.

[7] B.F. Levine. Quantum-well infrared photodetectors. *Journal of Applied Physics*, 74(8):R1–R81, October 1993.

[8] M. Ershov and H.C. Liu. Low-frequency noise gain and photocurrent gain in quantum well infrared photodetectors. *Journal of Applied Physics*, 86(11):6580–6585, December 1999.

[9] K.K. Choi. *The Physics of Quantum Well Infrared Photodetectors*. World Scientific Publishing Co. Pte. Ltd., 1997.

[10] B.F. Levine, A. Zussman, S.D. Gunapala, M.T. Asom, J.M. Kuo, and W.S. Hobson. Photoexcited escape probability, optical gain and noise in quantum well infrared photodetectors. *Journal of Applied Physics*, 72(9):4429–4443, November 1992.

[11] H.S. Nalwa, editor. *Handbook of Nanostructure Materials and Nanotechnology; Opyical Properties*, volume 4. Academic Press, 2000.

[12] P. Kruck, M. Helm, T. Fromherz, G. Bauer, J.F. Nutzel, and G. Abstreiter. Medium-wavelenght, normal-incidence, p-type Si/SiGe quantum well infrared photodetector with background limited performance up to 85 k. *Applied physics letters*, 69(22):3372–3374, November 1996.

[13] R. People, J.C. Bean, G.C. Bethea, S.K. Sputz, and L.J. Peticolas. Broadband (8-14 μm), normal incidence, pseudomorphic Ge_xSi_{1-x}/Si strained-layer infrared photodetector operating between 20 and 77 k. *Applied Physics Letters*, 61(9):1122–1124, August 1992.

[14] M.A. Gadir, P. Harrison, and R.A. Soref. Arguments for p-type $Si_{1-x}Ge_x$/Si quantum well photodetectors for the far and very-far (terahertz) infrared. *The Journal of Superlattices and Microstructures*, 2001. Accepted for publication.

[15] H.C. Liu and F. Capasso, editors. *Intersubband Transitions in Quantum Wells: Physics and Device Application 1; Semiconductors and semimetals*, volume 62, page 220 and 222 Academic Press, 2000.

[16] N.E.I. Etteh and P. Harrison. Carrier scattering approach to the origins of the dark current in mid- and far-infrared (terahertz) quantum-well intersubband photodetectors (QWIPs). *IEEE Journal of Quantum Electronics*, 37(5):672, May 2001.

[17] N.E.I. Etteh and P. Harrison. Full quantum mechanical scattering model of the dark current in quantum well intersubband photodetectors (QWIPs): The absence of sequaential tunneling and in-plane wavefunction decoherence. *IEEE Journal of Quantum Electronics*, pages 34–37, 2001.

[18] N.E.I. Etteh and P. Harrison. First principles calculations of the dark current in quantum well infrared photodetectors (QWIPs). *Physica E - Low-Dimensional Systems & Nanostructures*, 2001. MSS10 Conference, Johannes Kelper Uni., Linz, Austria - Submitted on 20th July.2001.

[19] M.A. Gadir, P. Harrison, and R.A. Soref. The advantages of p-type and design methodologies for $Si_{1-x}Ge_x$ far-infrared (terahertz) quantum well infrared photodetectors (QWIPs).

Physica E - Low-Dimensional Systems & Nanostructures, 2001. MSS10 Conference, Johannes Kelper Uni., Linz, Austria - Submitted on 20th July.2001.